

Western  Graduate&PostdoctoralStudies

Western University
Scholarship@Western

Electronic Thesis and Dissertation Repository

10-4-2012 12:00 AM

Comparison Between Three Types of Cable Stayed Bridges Using Structural Optimization

Olfat Sarhang Zadeh
The University of Western Ontario

Supervisor
Dr. Ashraf El Damatty
The University of Western Ontario

Graduate Program in Civil and Environmental Engineering
A thesis submitted in partial fulfillment of the requirements for the degree in Master of Engineering Science
© Olfat Sarhang Zadeh 2012

Follow this and additional works at: <https://ir.lib.uwo.ca/etd>

 Part of the [Structural Engineering Commons](#)

Recommended Citation

Sarhang Zadeh, Olfat, "Comparison Between Three Types of Cable Stayed Bridges Using Structural Optimization" (2012). *Electronic Thesis and Dissertation Repository*. 897.
<https://ir.lib.uwo.ca/etd/897>

This Dissertation/Thesis is brought to you for free and open access by Scholarship@Western. It has been accepted for inclusion in Electronic Thesis and Dissertation Repository by an authorized administrator of Scholarship@Western. For more information, please contact wlsadmin@uwo.ca.

COMPARISON BETWEEN THREE TYPES OF
CABLE STAYED BRIDGES USING STRUCTURAL
OPTIMIZATION

(THESIS FORMAT: INTEGRATED ARTICLES)

by

Olfat Sarhang Zadeh

Faculty of Engineering
Department of Civil and Environmental Engineering

Submitted in partial fulfillment
of the requirements for the degree of
Master of Engineering Science

School of Graduate and Postdoctoral Studies
The University of Western Ontario
London, Ontario, Canada
4 October, 2012

© Olfat Sarhang Zadeh 2012

Certificate of Examination

Western University

School of Graduate and Postdoctoral Studies

Supervisor

Examining Board

Dr. Ashraf El Damatty

Dr. Jon Southen

Dr. Girma Bitsuamlak

Dr. Robert Klassen

The thesis by

Olfat Sarhang Zadeh

entitled:

**Comparison Between Three Types of Cable-Stayed
Bridges Using Structural Optimization**

is accepted in partial fulfillment of the

requirements for the degree of

Master of Engineering Science

October 2012

Date

Chair of The Thesis Examining Board

Abstract

Cable stayed bridges have good stability, optimum use of structural materials, aesthetic, relatively low design and maintenance costs, and efficient structural characteristics. Therefore, this type of bridges are becoming more and more popular and are usually preferred for long span crossings compared to suspension bridges. A cable-stayed bridge consists of one or more towers with cables supporting the bridge deck. In terms of cable arrangements, the most common type of cable stayed bridges are fan, harp, and semi fan bridges. Because of their large size and nonlinear structural behaviour, the analysis of these types of bridges is more complicated than conventional bridges. In these bridges, the cables are the main source of nonlinearity. Obtaining the optimum distribution of post-tensioning cable forces is an important task and plays a major role in optimizing the design of cable stayed bridges. An optimum design of a cable-stayed bridge with minimum cost while achieving strength and serviceability requirements is a challenging task.

In this thesis, an advanced and comprehensive numerical model is used to obtain the post-tensioning forces and the optimum design of the three types of cable-stayed bridge. The numerical method is based on finite element, B-spline curves, and real coded genetic algorithm. The optimization accounts for all the variables that define the geometry and cross-section of the bridge. Comparison between the three types, in terms of post-tensioning forces and cost, is carried out in this thesis.

Keywords: Cable-Stayed Bridge, Finite Element, Fan Bridge, Semi Fan Bridge, Harp Bridge, Real Coded Genetic Algorithms, Genetic Algorithms, B-spline Function, Post-Tensioning Cable Forces, Optimization.

Dedication

To Reza and Ava.

To my parents.

Acknowledgements

All praise is due to God. I would like to express my appreciation and gratitude to Prof. Ashraf El Damatty for supervising my research during my M.E.Sc studies at Western University. I also would like to thank Dr. Mahmoud Hassan, for his suggestions, comments, and sharing his knowledge with me. I would like to thank my lab-mates and our research group.

Last but not least, I am grateful to my husband, for his love, and kind support during working on this research. I would like to thank my parents. I would like to thank my sisters, Ara, and Mitra for their wisdom and moral supports.

Contents

Certificate of Examination	ii
Abstract	iii
Dedication	iv
Acknowledgements	v
Contents	vi
List of Tables	x
List of Figures	xi
List of Algorithms	xiv
Nomenclature	xv
1 Introduction and Literature Review	1
1.1 Introduction	1
1.2 Background of Long Span Bridges	2
1.2.1 Suspension Bridges	2
1.2.2 Cable-Stayed Bridges	2
1.2.2.1 Harp arrangement	5

1.2.2.2	Fan arrangement	5
1.2.2.3	Semi-fan arrangement	6
1.3	Literature Review	7
1.4	Motivation and Problem Statement	9
1.5	Objectives of the Thesis	9
1.6	Thesis Outline	10
Bibliography		11
2 Comparison of Post-tensioning Cable Forces Between Three types of the Cable-stayed Bridges		15
2.1	Introduction	15
2.2	Description of the Reference Bridge	19
2.3	Numerical Model	21
2.3.1	Finite Element Model	21
2.3.1.1	Modeling the Stay Cables	21
2.3.1.2	Modeling the Pylon and Deck	23
2.3.2	B-Spline Curves	24
2.3.3	Design Variables and Objective Function	26
2.3.4	Real Coded Genetic Algorithm	28
2.3.4.1	Genetic Operators	30
2.3.5	Optimum Post-tensioning Cable Forces Algorithm	30
2.4	Post-tensioning Cable Forces for Three Cable Arrangements of Cable-Stayed Bridges	31
2.4.1	Post-tensioning Cable Forces for Three Cable Arrangements of Quincy Bayview Bridge	31

2.4.2	The Effect of Height of the Pylon on the Distribution of Post-tensioning Cable Forces with $n = 7$, $h = \{20, 40, 60\}$, and $M = 260$	34
2.4.3	The Effect of Mid-span Length on the Distribution of Post-tensioning Cable Forces with $n = 7$, $h = 20$, and $M = \{260, 270, 280\}$	36
2.4.4	The Effect of Number of Cables on the Distribution of Post-tensioning Cable Forces with $n = \{7, 10\}$, $h = \{20\}$, and $M = \{260\}$	39
2.5	Conclusion	40
Bibliography		42
3	Optimal Design of Harp, Fan, and Semi Fan Cable-Stayed Bridges	46
3.0.1	Design Variables	48
3.0.2	Design Constraints	53
3.0.2.1	Stay cables	53
3.0.2.2	Composite Concrete-Steel Deck	54
3.0.2.3	Pylon	56
3.1	Optimal Design Scheme	57
3.1.1	Objective Function	57
3.1.2	Finite Element Model	58
3.1.3	Real Coded Genetic Algorithm	59
3.1.4	Post-tensioning Cable Forces	60
3.1.5	Load Considerations	60
3.1.5.1	Dead Load	60
3.1.5.2	Live Load	61
3.1.5.3	Wind Load	61
3.1.5.4	Load Factors and Combinations	63

3.1.6	The Cost Optimization Algorithm	63
3.1.7	Description of the Bridge for Semi-fan, Fan and Harp Arrangement	65
3.2	Results	68
3.2.1	Reference Costs of Quincy Bayview Bridge	68
3.2.2	Comparison of the Optimal Cost of Different Arrangements	70
3.2.3	Effect of Geometric Configuration on the Bridge Cost	71
3.2.3.1	Effect of Geometric Configuration on the Pylon Cost	71
3.2.3.2	Effect of Geometric Configuration on the Deck Cost	73
3.2.3.3	Effect of Geometric Configuration on the Cables Cost	78
3.2.3.4	Effect of Geometric Configuration on the Bridge Cost	79
3.2.4	Effect of Number of Cables on the Bridge Cost	82
3.2.4.1	Effect of Number of Cables on the Pylon Cost	83
3.2.4.2	Effect of Number of Cables on the Deck Cost	84
3.2.4.3	Effect of Number of Cables on the Cables Cost	85
3.2.4.4	Effect of Number of Cables on the Bridge Cost	85
3.3	Conclusions	86
	Bibliography	88
4	Summary of the Thesis	92
4.1	Thesis Contributions	92
4.2	Future Work	95
	Bibliography	96
	Vita	100

List of Tables

2.1	The main parameters of the Quincy Bayview Bridge cable-stayed bridge with semi-fan arrangement.	21
3.1	Three factors define thickness of steel main girders [Clause 10.9.2 ,CAN/CSA-S6-2006]	50
3.2	Lower and upper bounds of the design variables	50
3.3	Material Properties of the bridge	67
3.4	Reference Cost of Quincy Bayview Bridge(Hassan, 2010)	69
3.5	Comparison of the optimal solutions for three types of the cable-stayed bridges	72
3.6	Parameters used to study effect of geometric configuration on the bridge cost.	73

List of Figures

1.1	A simple illustration of typical cable-stayed bridge.	3
1.2	Composite deck	4
1.3	Three main types of cable stayed brides.	6
2.1	Street view of the Quincy Bayview Bridge Wilson and Gravelle (1991) obtained from Google map.	19
2.2	Geometry of the Quincy Bayview Bridge	20
2.3	Finite Element Model of three type of the cable-stayed Bridge	22
2.4	B-spline curve	25
2.5	Representation of cable forces in a fan arrangement using B-spline curves.	26
2.6	Representation of cable forces in a harp arrangement using B-spline curves.	27
2.7	Distribution of cable forces in Bayview Bridge	32
2.8	Bending moment of the pylon in Bayview Bridge.	34
2.9	The post-tensioning stay cable forces for three main types of cable- stayed bridges with constant number of cables ($n = 7$), constant mid- span length ($M = 260$) and variable upper strut height ($h = 20, 40, 60$).	35
2.10	The post-tensioning stay cable forces for three main types of cable- stayed bridges with constant number of cables ($n = 7$), constant mid- span length ($M = 260, 270, 280$ m) and variable upper strut height ($h = 20$).	37

2.11	The post-tensioning stay cable forces for three main types of cable-stayed bridges with variable number of cables ($n = 7, 10$), constant mid-span length ($M = 260$ m), and constant height of the pylon ($h = 20$ m).	38
3.1	Geometry of three arrangement of cable-stayed bridges	51
3.2	Bridge deck cross section (a) Cross-section of the bridge deck for three arrangement of cable-stayed bridges and (b) Steel main girder.	52
3.3	Pylon elevation of three arrangement of cable-stayed bridges (a) Pylon elevation for semi-fan (b) Pylon elevation for harp and fan (c) Pylon cross-section.	52
3.4	Interaction diagram of deck.	55
3.5	Live load cases used in the numerical model(Hassan et al., 2012).	62
3.6	Alternative arrangements of Quincy Bayview Bridge	66
3.7	Variation of pylon cost with height of the pylon and main span length in fan and harp arrangements. Note that $N = 7$ and $\gamma_1 = \frac{M}{L} \in \{0.48, 0.50, 0.52, 0.54\}$	73
3.8	Variation of deck cost with height of the pylon and main span length for the semi-fan arrangement.	74
3.9	Variation of deck cost with height of the pylon and main span length for the fan and harp arrangements. Note that $N = 7$, $\gamma_1 = \frac{M}{L} \in \{0.48, 0.50, 0.52, 0.54\}$, and $\gamma_2 = \frac{h_B}{L} \in \{0.037, 0.055, 0.074, 0.11\}$	75
3.10	Variation of stay cables cost with height of the pylon and main span length for semi-fan arrangement.	76
3.11	Variation of stay cables cost with height of the pylon and main span length for the harp and fan arrangements. Note that $N = 7$, $\gamma_1 = \frac{M}{L} \in \{0.48, 0.50, 0.52, 0.54\}$, and $\gamma_2 = \frac{h_B}{L} \in \{0.037, 0.055, 0.074, 0.11\}$	77

3.12	Variation of bridge cost with height of the pylon and main span length for semi-fan arrangement.	80
3.13	Variation of bridge cost with height of the pylon and main span length for the fan and harp arrangements. Note that $N = 7$, $\gamma_1 = \frac{M}{L} \in \{0.48, 0.50, 0.52, 0.54\}$, and $\gamma_2 = \frac{h_B}{L} \in \{0.037, 0.055, 0.074, 0.11\}$	81
3.14	Variation of Pylon cost with number of stay cables in three types of cable-stayed bridges. Note that $N = \{5, 6, 7, 8, 9, 10, 11, 12, 13, 14\}$, $\gamma_1 = 0.52$, and $\gamma_2 = 0.083$	83
3.15	Variation of deck cost with number of stay cables in three types of cable-stayed bridges. Note that $N = \{5, 6, 7, 8, 9, 10, 11, 12, 13, 14\}$, $\gamma_1 = 0.52$, and $\gamma_2 = 0.083$	84
3.16	Variation of cables cost with number of stay cables in three types of cable stayed-bridges. Note that $N = \{5, 6, 7, 8, 9, 10, 11, 12, 13, 14\}$, $\gamma_1 = 0.52$, and $\gamma_2 = 0.083$	85
3.17	Variation of total cost with number of stay cables in three types of cable-stayed bridges. Note that $N = \{5, 6, 7, 8, 9, 10, 11, 12, 13, 14\}$, $\gamma_1 = 0.52$, and $\gamma_2 = 0.083$	86

List of Algorithms

2.1	Optimum Post-tensioning Cable Forces Algorithm	29
3.1	Modified Optimum Cost Design Algorithm Hassan et al. (2012) . . .	64

List of Abbreviations

DOF	Degree of Freedom
ULM	Unit Load Method
FEM	Finite Element Model
GA	Genetic Algorithm
CGA	Coded Genetic Algorithm
PDE	Partial Differential Equations
RCGA	Real Coded Genetic Algorithm

Chapter 1

Introduction and Literature Review

1.1 Introduction

THE history of cable stayed bridges dates back to 1595, found in a book by the Venetian inventor (Bernard et al., 1988). Many suspension and cable-stayed bridges have been designed and developed since 1595 such as the Albert bridge and the Brooklyn bridge (Wilson and Gravelle, 1991), (Bernard et al., 1988). Cable-stayed bridges have been later constructed all over the world. The Swedish Stromsund bridge, designed in 1955, is known as the first modern cable-stayed bridge (Wilson and Gravelle, 1991). The total length of the bridge is 332 m, and its main span length is 182 m. It was opened in 1956, and it was the largest cable-stayed bridge of the world at that time. This bridge was constructed by Franz Dischinger, from Germany, who was a pioneer in construction of cable-stayed bridges (Tori et al., 1968). The designers realized that cable stayed style requires less material for cables and deck and can be erected much easier than suspension bridges (Bernard et al., 1988), (Tori et al., 1968), (Wilson and Gravelle, 1991), (Simoes and Negrao, 1994), (Ren and Peng, 2005), and (Nieto et al., 2009). This is mainly due to advances in design and construction method and the availability of high strength steel cables. The Theodor

Heuss bridge was the second true cable-stayed bridge and was erected in 1957 across the Rhine river at Dusseldorf. It had a main span of 260 m and side spans of 108 m which was larger than the Stromsund. It has a harp cable arrangement with parallel stays and a pylon composed of two free-standing posts fixed to the deck. The reason for choosing the harp style was aesthetics appearance. The Severins Bridge in Köln designed in 1961 was the first fan shape cable stayed bridge, which has a A-shape pylon. In this bridge, the cross section of the deck was similar to the one used in Theodor Heuss bridge (Bernard et al., 1988). The Flehe bridge was the first semi-fan type which was erected in 1979 in Dusseldorf, Germany over the Rhine river. The remarkable feature of this bridge was the reinforced concrete tower, which has the shape of an inverted Y (Bernard et al., 1988). In what follows, the main types of long span bridges are reviewed.

1.2 Background of Long Span Bridges

There are two main types of long span bridges: suspension bridges and cable stayed bridges.

1.2.1 Suspension Bridges

A suspension bridge is a type of bridge in which the deck, i.e., load bearing part, hangs below suspension cables using vertical suspenders. The vertical suspenders carry the weight of the deck.

1.2.2 Cable-Stayed Bridges

A typical cable stayed bridge is a deck with one or two pylons erected above the piers in the middle of the span. The cables are attached diagonally to the girder to provide additional supports. A typical cable-stayed bridge is depicted in Fig. 1.1. The pylons

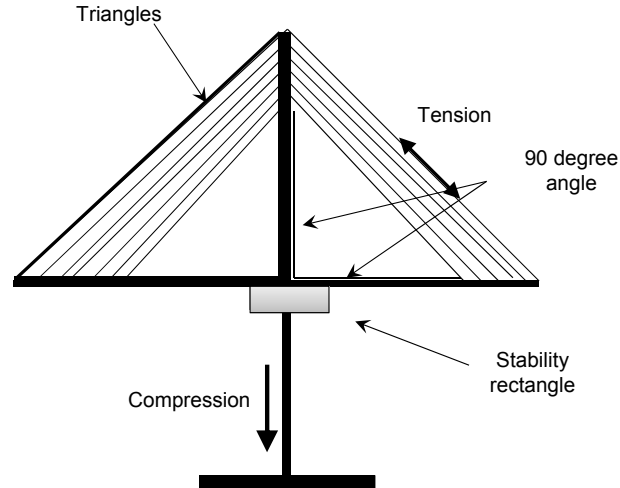


Figure 1.1: A simple illustration of typical cable-stayed bridge.

form the primary load-bearing structure in these types of bridges. Large amounts of compression forces are transferred from the deck to the cables to the pylons and into the foundation as shown in Fig. 1.1. The design of the bridge is conducted such that the static horizontal forces resulting from dead load are almost balanced to minimize the height of the pylon. Cable stayed-bridges have a low center of gravity, which makes them efficient in resisting earthquakes. Cable stayed bridges provide outstanding architectural appearance due to their small diameter cables and unique overhead structure.

A cable stayed bridge is composed of three main components as explained below.

Deck

The deck or road bed is the roadway surface of a cable-stayed bridge. The deck can be made of different materials such as steel, concrete or composite steel-concrete. The choice of material for the bridge deck determines the overall cost of the construction of cable stayed bridges. The weight of the deck has significant impact on the required stay cables, pylons, and foundations (Bernard et al., 1988). As one can see in Fig. 1.2, the composite steel-concrete deck is composed of two structural edge girders. These girders are attached by transverse steel floor beams. The precast reinforced concrete

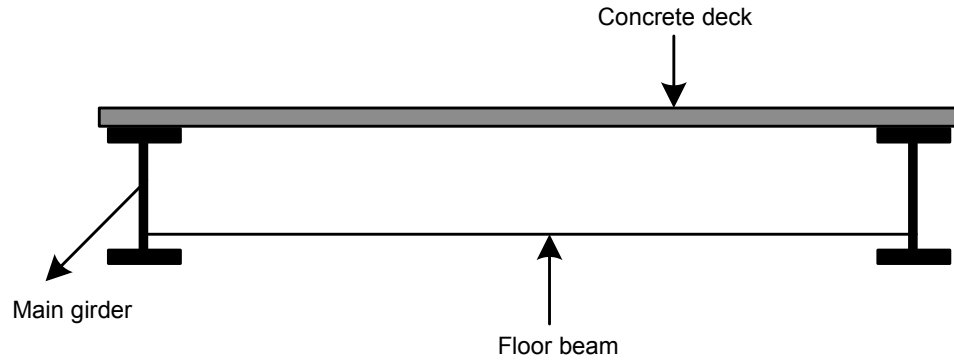


Figure 1.2: Composite deck

deck is supported by these two main girders. This type of composite steel-concrete deck has more advantages as follow (Hassan et al., 2012):

- The own weight of a composite deck is less than a concrete deck.
- The light steel girders can be erected before applying the heavy concrete slab.
- The stay cables have more resistance against rotation anchoring to the outside steel main girders.
- The redistribution of compression forces due to shrinkage and creep onto the steel girders is minimized by using the precast slab.

Pylon

Pylons of cable stayed bridges are aimed to support the weight and live load acting on the structure. There are several different shapes of pylons for cable stayed bridges such as Trepezoidal pylon, Twin pylon, A-frame pylon, and Single pylon. They are chosen based on the structure of the cable stayed bridge (for different cable arrangements), aesthetics, length, and other environmental parameters.

Cables

Cables are one of the main parts of a cable-stayed bridge. They transfer the dead weight of the deck to the pylons. These cables are usually post-tensioned based on the weight of the deck. The cables post-tensioned forces are selected in a way to minimize both the vertical deflection of the deck and lateral deflection of the pylons. There are four major types of stay cables including, parallel-bar, parallel-wire, standard, and locked-coil cables. The choice of these cables depends mainly on the mechanical properties, structural properties and economical criteria.

In what follows, different types of cable-stayed bridges are discussed based on the arrangement of stay cables including harp, fan, and semi-fan as depicted in Fig. 1.3.

1.2.2.1 Harp arrangement

In a harp arrangement, the cables are made nearly parallel by attaching them to different points on the pylon as shown in Fig. 1.3a. From an economical point of view, this type of cable-stayed bridge is not efficient for long span bridges. This is because such an arrangement requires more steel for the cables, gives more compression in the deck, and produces bending moments in the pylon. However, in terms of aesthetics it is attractive in comparison to other types of cable-stayed bridges. The parallel cables give a most pleasant appearance to the harp arrangement as stated by Bernard et al. (1988). The need for taller pylons is one of the disadvantages of this type of cable-stayed bridge.

1.2.2.2 Fan arrangement

In this pattern, all the stay cables are attached to a single point at the top of each pylon as shown in Fig. 1.3b. The relatively steep slope of the stay cables results in a smaller cable cross section in comparison to the harp type. Moreover, the horizontal cable forces in the deck in this arrangement are less than the harp type (Bernard et al., 1988).

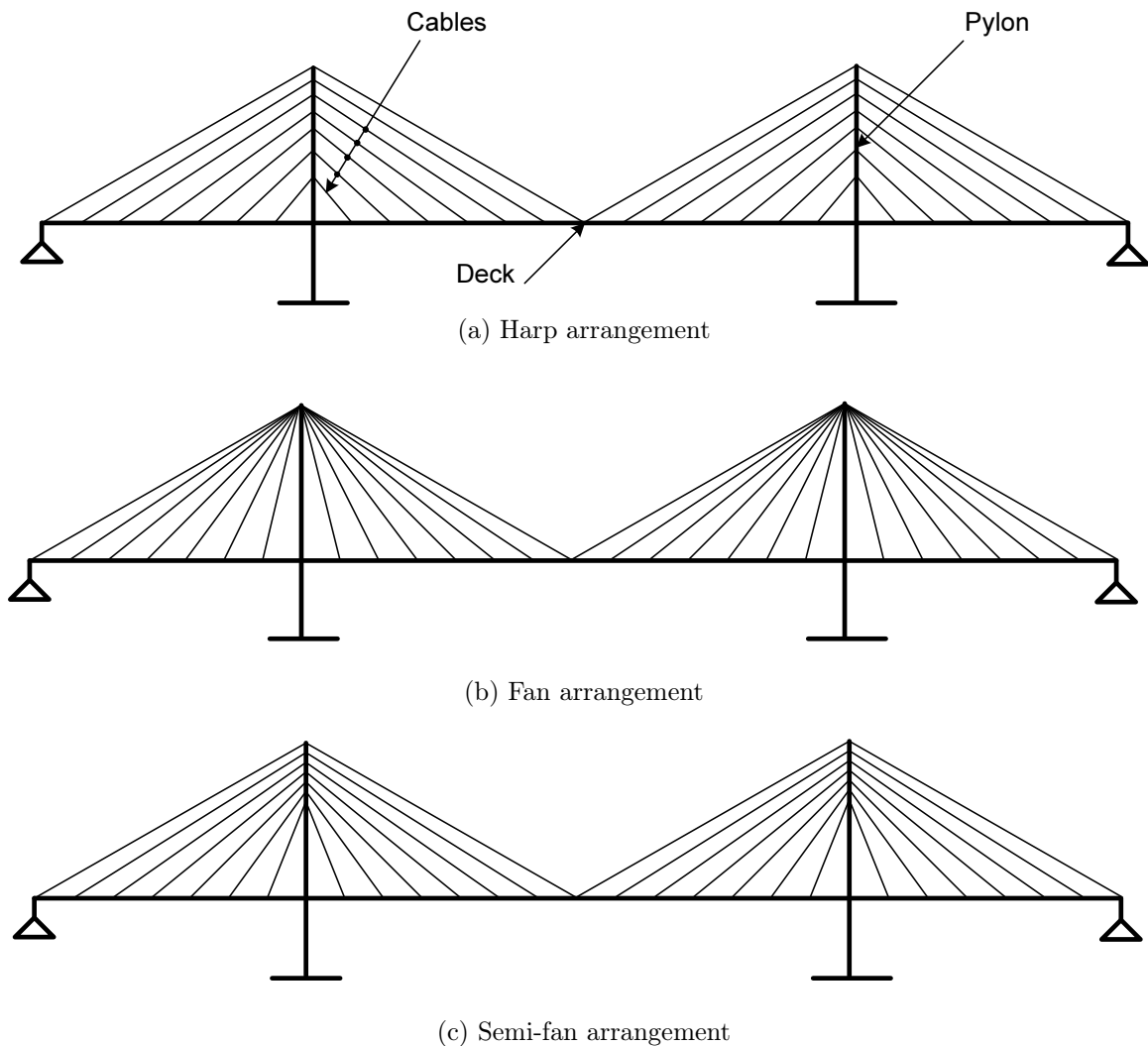


Figure 1.3: Three main types of cable stayed bridges.

However, by increasing the number of the stay cables, the weights of the anchorages increase and attaching the stay cables to anchorage becomes difficult. Therefore, the fan patterns are suitable only for moderate spans with a limited number of stay cables.

1.2.2.3 Semi-fan arrangement

Several modern cable-stayed bridges have been built around the world using semi-fan arrangement due to its efficiency. As shown in Fig. 1.3c, in this system, the cables

are distributed over the upper part of the pylon, which are more steeply inclined close to the pylon (Bernard et al., 1988). The world largest cable-stayed bridge (Sutong Bridge in Jiangsu, China) was designed as a semi-fan arrangement using A-shape pylons. The semi-fan arrangement has better appearance in comparison to the fan arrangement.

1.3 Literature Review

In this section, a brief review of the previous works on optimum design of cable stayed bridges available in the literature is given.

Simoes and Negro (1994) proposed an entropy-based scheme for cost optimization of cable stayed bridges. In this method, the post-tensioning cable forces are not included in this analysis and the number of stay cables as well as the length of the the span are assumed to be constant.

Long et al. (1999), has employed an efficient algorithm based on internal penalty algorithm to optimize the cost of cable-stayed bridges. Similar to the scheme presented by Simoes and Negro (1994), the pylon height, span length, and the number of stay cables received a pre-assigned value. Also, in this work the effect of post-tensioning forces of cable stays has not been considered in the optimization method.

A convex scalar function has been employed to optimize the cost of the deck in cable-stayed bridges by Simoes and Negro (2000). In this scheme, post-tensioning forces of stay cables are also considered. The convex scalar function combines the dimensions of the bridge and the post-tensioning cable forces. Note that in this scheme pylon height and span length are not considered as design variables in this optimization technique.

Jajnic et al. (2003), presented an efficient scheme to find optimal tensioning strategy for the construction of cable-stayed bridges in which three main sources of non-

linearities are considered. Also, bending moment distribution at the deck connections is used to find the optimum cable forces.

Sung et al. (2006) studied optimum post-tensioning cable forces for cable-stayed bridges. It is shown that the upper limits on cable forces for the cable-stayed bridges are due to a dead load. In this work, post-tensioning forces of stay cables are taken into account. The Mau-Lo Hsi cable-stayed bridge located in Taiwan is considered as a case study.

Lee et al. (2008), proposed an optimization of tensioning strategy for asymmetric cable-stayed bridge and its effect on the construction process. Unit load method (ULM) is considered as it can take into account the actual construction process while other approaches are based on configuration of the final structure only. The numerical results are given to show the validity of the proposed approach.

A scheme based on genetic algorithm is incorporated for optimizing the cable-stayed bridges by Lute et al. (2009). The computation time of the genetic algorithm has been reduced employing a support vector machine. In this method, the number of stay cables is assumed to be constant. Moreover, the effect of post-tensioning cable forces has not been considered in this optimization scheme.

Most recently, Baldomir et al. (2010) investigated cable optimization of long span cable-stayed bridges. The cross section of stay cables as well as constraint of cable stress and deck displacement is considered.

Zhang and Wu (2011) used an optimization method of unknown load factor to determine the cable forces to achieve an ideal state. Then, the ideal cable forces are established and a construction stage analysis is performed.

The current study is based on the recent work conducted by Hassan et al. (2012) a new technique for optimal design of cable-stayed bridges with semi-fan arrangements based on a finite element model, B-spline curves, and real coded genetic algorithm.

1.4 Motivation and Problem Statement

Optimal design of cable-stayed bridges has a lot of potentials to reduce the cost of the bridges. In cable-stayed bridges, there are many parameters that one should consider such as: (a) horizontal distance from the pylon to the point of attachment on the deck, (b) height of point of attachment above the bridge level, (c) length of the stay cables, and (d) angle between the cables and the pylons. Therefore, there are several compromises in the design of a cable-stayed bridge based on the arrangements that one may choose. Moreover, optimizing the design cost of cable-stayed bridges using post-tensioning cable forces is crucial.

In all of the previous work presented in Section 1.3, a comprehensive comparison among the major types of cable-stayed bridges is missing. It is not clear which type, i.e., fan, harp, or semi-fan, can provide the optimal cost in these bridges. In the work presented by Hassan et al. (2012), only the post-tensioning cable forces and optimal design cost for the design of semi-fan arrangement is considered. This work uses finite element analysis, B-spline curves, and real coded genetic algorithm to achieve the optimal cable forces.

1.5 Objectives of the Thesis

In this thesis, a new method to obtain post-tensioning cable forces for cable-stayed bridges is employed. The main objectives of this thesis are:

- To determine the optimum post-tensioning cable forces for three types of cable-stayed bridges with fan, semi-fan, and harp arrangements under the action of dead load.
- To compare post-tensioning cable forces between fan, semi-fan, and harp arrangements.

- To determine optimum design cost of three arrangements of cable-stayed bridges based on the numerical method and comparing them to each other.

This thesis also provides comparison to its counterpart (the semi-fan cable-stayed bridge) which has been recently published by Hassan et al. (2012). Also, it should be noted that the techniques used in this thesis are based on the one proposed by Hassan (2010).

1.6 Thesis Outline

This thesis is prepared in monograph format and is organized as follows. In present chapter, a literature review on some of the existing works in the literature on optimal design of cable-stayed bridges is provided.

In Chapter 2, a numerical method based on finite element model, B-spline curves and genetic algorithm is used to obtain the optimum post-tensioning cable forces for the fan and harp arrangements of cable-stayed bridges. Also, the obtained cable forces are compared with each other and the semi-fan arrangement as the counterpart. The post-tensioning cable forces are determined for various pylon heights, deck length, and number of stay cables.

In Chapter 3, based on the post-tensioning cable forces obtained in Chapter 2, and the numerical methods including finite element analysis, B-spline curves, and real coded genetic algorithm, the optimum cost of fan and harp arrangement of cable-stayed bridges are determined. Also, the results are compared with the counterparts available in the literature including semi-fan arrangement proposed by Hassan et al. (2012) and the reference bridge.

Finally, in Chapter 4, the contributions are summarized and possible directions for future works are provided.

Bibliography

- M. Hassan. *Optimum Design of Cable-Stayed Bridges*. PhD thesis, The University of Western Ontario, 2010.
- John. Wilson and Wayne Gravelle. Modelling of A Cable-Stayed Bridge For Dynamic Analysis. *Journal of Earthquake Engineering and Structural Dynamics*, 20:707–771, 1991.
- M.M. Hassan, A. A. El Damatty, and Nassef. Determination of Optimum Post-Tensioning Cable Forces for Cable-stayed Bridges. *Journal of Engineering Structures*, in press, 2012.
- H. Bernard, Isler Walmer, and Moia Pierre, editors. *Cable Stayed Bridges*. Presses Polytechniques Romandes, Lausanne, Switzerland, 1988. ISBN 0-7277-1321-3.
- K. Tori, K. Ikeda, and T Nagasaki. A Non-iterative Optimum Design Method for Cable-Stayed Bridges. In *Proceedings of Japan Society of Civil Engineers*, pages 115–123, 1968.
- LMC. Simoes and JHJO Negroao. Sizing and Geometry Optimization of Cable-stayed Bridges. *Journal of Computer and Structure*, 52:309–321, 1994.
- W.X. Ren and X.L. Peng. Baseline finite element modeling of a large span cable-stayed bridge through field ambient vibration tests. *Computers & structures*, 83(8):536–550, 2005.

- F. Nieto, S. Hernandez, and J A. Julardo. Optimum Design of Long-span Suspension Bridges Considering Aeroelastic and Kinematic Constraints. *Journal of Structure Multidisc. Optim.*, 39:133–151, 2009.
- W. Long, MS. Troitsky, and ZA Zielinski. Optimum Design of Cable Stayed Bridges. *Journal of Structural Engineering and Mechanics*, 7:241–257, 1999.
- LMC. Simoes and JHJO Negro. Optimization of Cable-Stayed Bridges with Box-girder Decks. *Journal of Advanced Engineering*, 31:417–423, 2000.
- D. Jajnic, M. Pircher, and H Pircher. Optimization of Cable Tensioning in Cable-Stayed Bridges. *Journal of Bridge Engineering*, 8:131–137, 2003.
- YU-CHi. Sung, Dyi-Wei. Chang, and Eng-Huat Teo. Optimum Post-Tensioning cable Forces of Manu-Lo Hsi Cable-Stayed Bridge. *Journal of Engineering Structures*, 28:1407–1417, 2006.
- T.Y. Lee, Y.H. Kim, and S.W. Kang. Optimization of tensioning strategy for asymmetric cable-stayed bridge and its effect on construction process. *Structural and Multidisciplinary Optimization*, 35(6):623–629, 2008.
- V. Lute, A. Upadhyay, and KK Singh. Computationally Efficient Analysis of Cable-stayed Bridges for GA-based Optimization. *Journal of Engineering Applied Artificial Intell.*, 22(4-5):750–758, 2009.
- A. Baldomir, S. Henandez, F. Nieto, and A Jurado. Cable Optimization of a Long Span Cable-Stayed Bridge in La Coura (Spain). *Journal of Advances in Engineering Software*, 41:931–938, 2010.
- Tao. Zhang and ZhiMin Wu. Dead Load Analysis of Cable-Stayed Bridge. In *International Conference on Intelligent Building and Management (CSIT'11)*, pages 270–274, 2011.

- PH. Wang, TC. Tseng, and CG Yang. Initial Shape of Cable Stayed Bridges. *Journal of Computational Structure*, (46):1095–1106, 1993.
- JH Ernst. Der E-Modul von Seilen unter berucksichtigung des Durchhanges. *Der Bauingenieur*, 40(2):52–59, 1965.
- AS. Nazmy and AM. Abdel-Ghaffar. Three-dimensional nonlinear static analysis of cable-stayed bridges. *Journal of Structural Engineering*, 34(2):257–271, 1990.
- W Jr Weaver and JM Gere, editors. *Matrix Analysis of Framed Structures*. 3rd Edn, New York: Van Nostrand Reinhold; 1980, 1980.
- M. Gen and R. Cheng, editors. *Genetic Algorithms and Engineering Optimization*. Wiley, NewYork, 2000. ISBN 0-7277-1321-3.
- M. Pourazaday and X. Xu. Direct Manipulations of B-spline and NURBS Curves. *Journal of Advances in Engineering Software*, 31(2):107–118, 2000.
- AM El Ansary, AA El Damatty, and AO Nassef. A coupled finite element genetic algorithm technique for optimum design of steel conical tanks. *Thin-Walled Structures*, 48(3):260–273, 2010.
- CAN/CSA-S6-06. Canadian highway bridge design code s6-06 (can/csa s6-06). *Canada: Canadian Standard Association, Ontario*, 2006.
- AASHTO.LRFD. Bridge Design Specifications. *4th Edition Washington D.C., USA*, 2007.
- L Davis, editor. *Handbook of Genetic Algorithms*. Van Nostrand Reinhold, New York, USA, 1991. ISBN 0-7277-1321-3.
- Z Michalewics and DB Fogel, editors. *How to Solve it: Modern Heuristics*. 2nd Edition, Springer, New York, USA, 2004.

R Walther, B Houriet, W Isler, P Moia, and JF Klein. Cable-Stayed Bridges. *Thomas Telford Ltd*, 1988.

MS Troitsky, editor. *Cable-Stayed Bridges: Theory and Design*. 2nd Edition, Oxford: BSP 1988, 1988.

Chapter 2

Comparison of Post-tensioning Cable Forces Between Three types of the Cable-stayed Bridges

2.1 Introduction

IN this chapter, the post-tensioning cable forces of cable-stayed bridges are evaluated for three arrangement of cable-stayed bridges. Three main types of cable-stayed bridges, fan, semi-fan, and harp are considered in this chapter. As explained in Chapter 1, cable-stayed bridges are large and realized as complicated structures. Recently, to address the design cost of cable-stayed bridges several researches have been performed and are available in the literature. For instance one can refer to Wilson and Gravelle (1991), Sung et al. (2006), Tori et al. (1968), Simoes and Negro (1994), Ren and Peng (2005), Nieto et al. (2009), and Zhang and Wu (2011). They cover various topics such as post-tensioning cable forces, efficient finite element modeling, and effect of dead load on the stay cables. The superstructure of cable-stayed bridges requires to post-tension the stay cables to improve the determinal influence of the

uniform loading due to dead load acting on the deck (Sung et al., 2006). Therefore, since cable-stayed bridges are not deterministic structures, then the solutions for the post-tensioning cable forces are not unique. This makes it difficult to find an optimal design for these bridges (Sung et al., 2006) and hence a comprehensive research should be performed to obtain the optimal post-tensioning cable forces in the cable-stayed bridges.

The determination of the optimum post-tensioning cable forces for an optimum structural performance is one of the important practice that needs to be considered in the design of cable-stayed bridges. In this effect, several researches in the literature have considered optimal design of stay-cables based on post-tensioning forces.

Tori et al. (1968), proposed a non-iterative optimal analysis to find the post-tensioning cable forces in cable-stayed bridges. A transformed objective function is obtained using the post-tensioning forces. Then, by zeroing the partial derivatives of the transformed objective function, the post-tensioning cable forces are determined (Sung et al., 2006).

Wang et al. (1993), proposed an iterative approach to find the solution of the post-tensioning cable forces. This method is repeated until the cable forces are determined and the precision of the displacements of the deck and pylon converges to an allowable threshold.

Most of the previously proposed schemes for post-tensioning optimization are based on two techniques. One is limiting the vertical deflections of the bridge deck to a threshold value and the other one is to obtain a bending moment diagram along the deck in such a way that the deck is resting at the cable locations.

Recently, Hassan et al. (2012), developed a novel method to determine the optimum distribution of post-tensioning cable forces under the action of dead load. This method minimizes both the vertical deflection of the deck and the lateral deflection of the pylons for semi-fan type cable-stayed bridges. In this approach, a combina-

tion of finite element model, B-spline functions, and versatile optimization algorithm (real coded Genetic algorithm) is incorporated. The post-tensioning cable forces for semi-fan type cable-stayed bridges are obtained and employed for the optimal design of this type of cable-stayed bridge. In the same study, the optimal design cost is compared with a reference semi-fan cable stayed bridge. It is noted that in the work conducted by Hassan et al. (2012), only semi-fan arrangement is considered.

In this study, the method proposed by Hassan et al. (2012) is adopted since it has many advantages over the previous works. In the following, summary of the advantages of the scheme proposed by Hassan et al. (2012) is provided:

- The cable forces are usually treated as discrete design variables in the standard post-tensioning optimization approaches. In cable-stayed bridges, as the number of stay cables is significant, the number of design variables becomes quite large and this can lead to potential numerical problems. B-spline curves are employed to represent the distribution of cable forces along the deck length (Hassan et al., 2012). The shape of the B-spline curves is defined by a fewer number of parameters which are considered as the design variables. The merit of employing B-spline curve is that the number of shape parameters is significantly less than the number of stay cables. Therefore, the number of design variables in the optimization process is decreased. This results in reduction of the complexity of the optimization search space, as well as the computational time. This method also increases the probability of finding the global optimum solution and improves the performance of the optimization technique.
- In the previously proposed schemes, the vertical deflections of the bridge deck are converged to a tolerance threshold. Then, a bending moment diagram along the deck is obtained in such a way that the deck is resting on simple rigid supports at the cable locations. In the approach adopted by Hassan et al. (2012), the behaviour of the pylon in the optimization procedure is considered

as well . Therefore, the objective function minimizes the transverse deflections of the deck and pylons' tops, simultaneously. As a result, the bending moment distributions along both the pylon and the deck are minimized.

- In long span cable-stayed bridges with a mid-span length more than 1000 m, a large number of stay cables is required. Therefore, the solution to the optimum post-tensioning cable forces is not unique and large sets of candidate solutions can exist within the search space. In the work done by Hassan et al. (2012), a global optimization method based on the Genetic Algorithm (GA) is used to optimize the shape of post-tensioning functions, which is capable of finding the global minimum of the optimization problem.

In the current study, finite element models for two other main types of cable-stayed bridges, i.e., fan and harp arrangements are developed. Then, the post-tensioning cable forces for these two arrangements of cable-stayed bridges are obtained. Moreover, the determined post-tensioning cable forces are compared to the one obtained for the semi-fan arrangement reported by Hassan et al. (2012). A comparison between the results of the post-tensioning cable forces for fan, semi-fan, and harp arrangements is illustrated. Finally, The effect of upper strut height, mid-span length, and the number of stay cables on the post-tensioning cable forces are investigated.

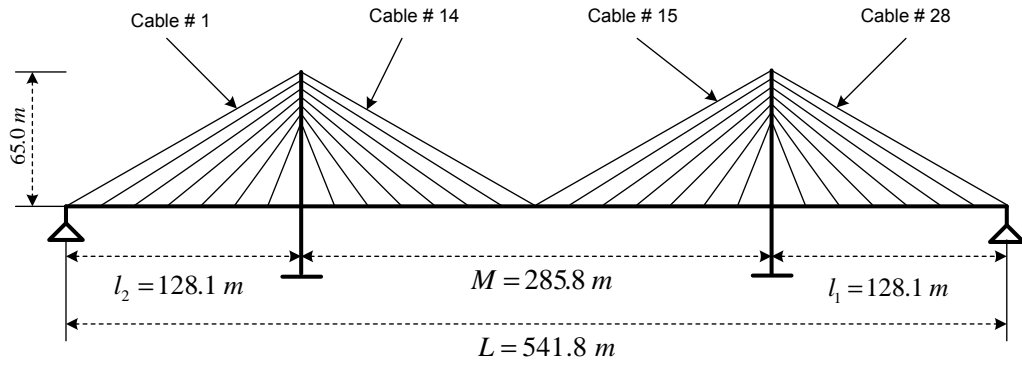
The rest of this chapter is organized as follow: In Section 2.2, the explanation of the cable stayed bridge used as a case study is shown. In Section 2.3, the numerical model of the cable-stayed bridge for the three cable configurations is presented. Also, in this section, the details of the numerical model used including finite element scheme, B-spline function, and Genetic algorithm for optimization are illustrated. In Section 2.4, the post-tensioning cable forces for fan and harp arrangements are obtained and are compared with post-tensioning cable forces for semi-fan arrangement. Finally, in Section 2.5, the main conclusions obtained from the study are summarized.



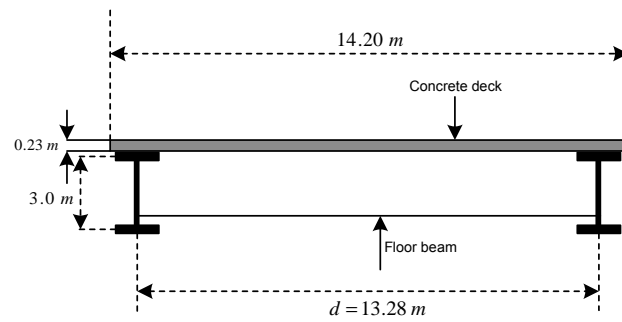
Figure 2.1: Street view of the Quincy Bayview Bridge Wilson and Gravelle (1991) obtained from Google map.

2.2 Description of the Reference Bridge

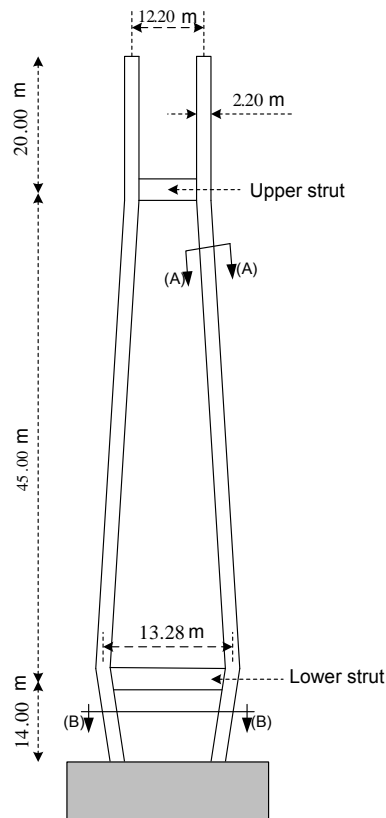
In this study, the Quincy Bayview Bridge located in Illinois, USA as shown in Fig. 2.1 is chosen as a typical cable-stayed bridge. The bridge is composed of 56 stay cables. The total length of the bridge $L = 541.8$ m with a main span length $M = 285.6$ m and two side spans $l_1 = l_2 = 128.1$ m as depicted in Fig. 2.2a. As one can see, in this figure the deck superstructure is supported by stay cables with a semi-fan arrangement. The precast concrete deck has a thickness of 0.23 m and a width of 14.2 m as illustrated in Fig. 2.2b. It also has two steel main girders that are located at the outer edge of the deck. These girders are internally attached by a set of equally spaced floor beams. The pylons have two concrete legs as they are connected internally with a pair of struts. The lower legs of the pylon are connected by a 1.12 m thick wall. Other geometric and parameters of the bridge are given in Table 2.1. The elevation view of this bridge is depicted in Fig. 2.2c. As one can see, the pylon has a H-shape with two concrete legs. The upper strut cross beam height is 45 m, and the lower strut cross beam supports the deck. The cross-section of the pylons is also given in Fig. 2.2d.



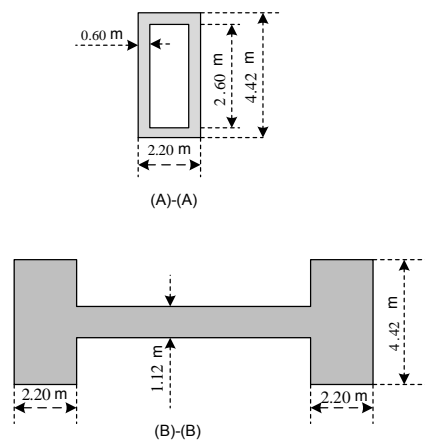
(a) Cable numbers and geometry of the bridge



(b) Cross section of the bridge deck



(c) Elevation view of the bridge pylon



(d) Cross section of the pylon

Figure 2.2: Geometry of the Quincy Bayview Bridge

Table 2.1: The main parameters of the Quincy Bayview Bridge cable-stayed bridge with semi-fan arrangement.

Bridge Parameter	Definition	Value
I_{dv}	Vertical moment of inertia of the deck	0.704 m ⁴
I_{dh}	Transverse moment of inertia of the deck	14.2 m ⁴
A_d	The cross-section area of the deck	0.602 m ²
E_{ds}	The modulus of elasticity of the deck	$2 \times 10^8 \frac{KN}{m^2}$
E_{cs}	The modulus of elasticity of the cables	$2.1 \times 10^8 \frac{KN}{m^2}$
T_{cCable}	The ultimate tensile strength of the cables	$1.6 \times 10^6 \frac{KN}{m^2}$
w_{cs}	The weight per unit length of the cables	$1.36 \frac{KN}{m}$
E_c	The modulus elasticity of the concrete	$2.5 \times 10^7 \frac{KN}{m^2}$

2.3 Numerical Model

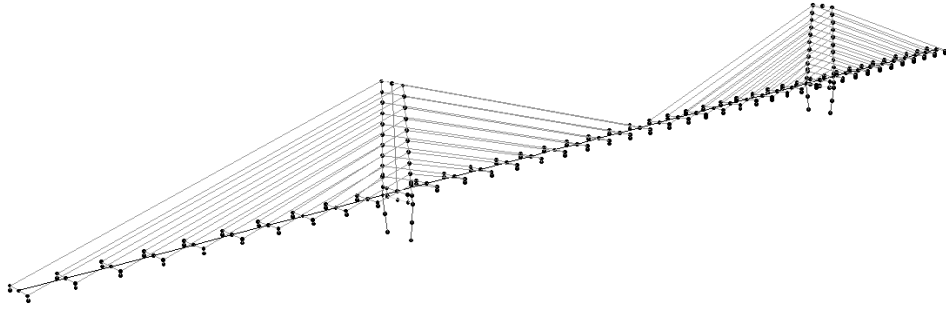
In this thesis, the numerical model developed by Hassan et al. (2012) is employed. The method is based on finite element modeling, B-spline functions, and Genetic algorithm (GA). In the following, a brief description for these three numerical techniques are provided.

2.3.1 Finite Element Model

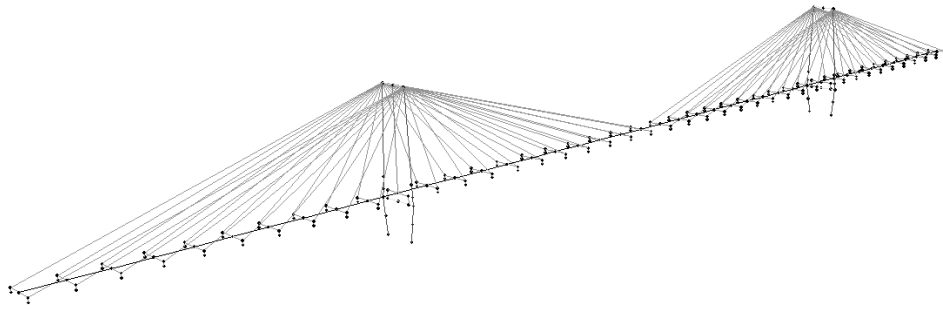
As explained in Chapter 1, cable-stayed bridges have three main components: Pylon or tower, deck, and the stay cables. These three components are modeled using three-dimensional line elements as shown in Fig. 2.3. To simulate the deck and the pylon, a three-dimensional nonlinear frame element is applied. Also, a three-dimensional nonlinear cable element is used to model the cables. In the following subsections, the modeling of these components is explained.

2.3.1.1 Modeling the Stay Cables

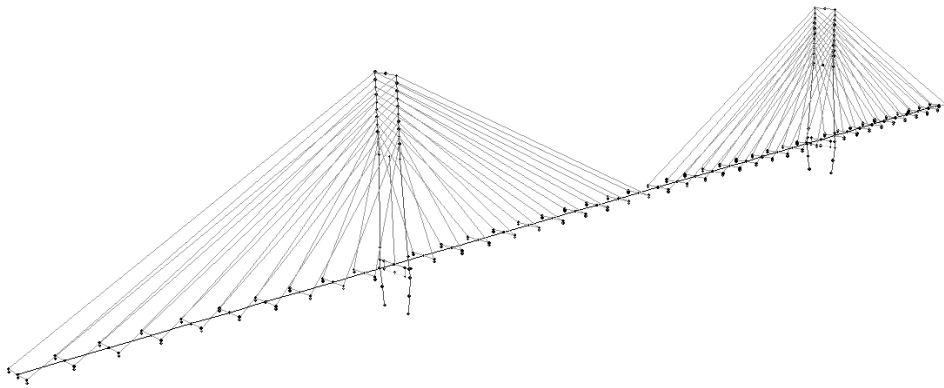
The axial stiffness of a stay cable changes non-linearly with cable tension and cable sagging. The equivalent modulus approach developed by Ren and Peng (2005) and Ernst (1965) is the most adopted method for modeling the stay cables. In this method,



(a) Finite Element Model of Harp type



(b) Finite Element Model of Fan type



(c) Finite Element Model of Semi-Fan type

Figure 2.3: Finite Element Model of three type of the cable-stayed Bridge

each cable is replaced by one truss element having equivalent cable stiffness. The equivalent tangent modulus of elasticity E_{eq} used to account for the sag effect is

$$E_{eq} = \frac{E_{cs}}{1 + \frac{(W_{cs}l)^2 AE}{12T^3}}, \quad (2.1)$$

where, E_{cs} is the cable material effective modulus, l is the horizontal projected length of a cable, w_{cs} is the weight per unit length of the cable, A is the cross-sectional area of the cable, and T is the tension in the cables.

2.3.1.2 Modeling the Pylon and Deck

For modeling the pylon, a three-dimensional non-linear scheme presented by Nazmy and Abdel-Ghaffar (1990) and Weaver and Gere (1980) is used. Let $[k_E]_b$ and $[k_G]_b$ be the elastic stiffness and geometric stiffness matrices of a 3D frame element, respectively. Then, the local tangent stiffness of a frame element $[k_T]_b$ that includes $P - \Delta$ and large displacement effects can be obtained from the work done by Weaver and Gere (1980) and Nazmy and Abdel-Ghaffar (1990) as

$$[k_T]_b = [k_E]_b + [k_G]_b. \quad (2.2)$$

To model the deck, the scheme proposed by Wilson and Gravelle (1991) is employed in this study. The deck is modeled using a single spine passing through its shear center. The translational and rotational stiffness of the deck are calculated and assigned to the frame elements of the spine. Also, a massless horizontal rigid link is incorporated to connect the cable anchorages and the deck spine to achieve the proper offset of the cables from the center-line of the deck. The finite element models of fan, semi-fan, and harp arrangements for cable-stayed bridges are illustrated in Fig. 2.3.

2.3.2 B-Spline Curves

The investigation of the distributions of the post-tensioning cable forces by Simoes and Negrao (2000), Gen and Cheng (2000), and Lee et al. (2008), along the span of a cable-stayed bridge, show that they follow an arbitrary polynomial function. This polynomial function can be represented by a p -th order polynomial as

$$f = a_1x^n + a_2x^{n-1} + a_3x^{n-2} + \dots + a_p \quad (2.3)$$

where f is the post-tensioning cable function, and x is the length of the bridge span. If such a function is used, the independent variables employed in the optimization technique are the coefficients a_i , $1 \leq i \leq p$. However, there are many limitations and disadvantages that arise when using power polynomial functions. It is hard to predict the proper range of values of such coefficients a_i for a specific optimization problem. The optimum function f has often a complicated shape that should be described by high order polynomials with a large number of coefficients.

In this study, B-spline curves are selected to represent the post-tensioning functions. B-spline curves are piecewise polynomials that remedy all the shortcomings associated with the power polynomial curves. They can be used to describe complex curves with lower-degree polynomials. Moreover, they have local control property that allows the user to modify a specific part of a curve and leaves the rest of the curve unchanged. These curves are well known mainly for shape optimization problems (Pourazaday and Xu, 2000). These curves are employed to represent the post-tensioning functions for semi-fan arrangements by Hassan et al. (2012).

As shown in Fig. 2.4, the p -th degree B-spline curve $C(u)$ can be defined as

$$C(u) = \sum_{i=0}^n N_{i,p}(u)P_i, \quad 0 \leq u \leq 1, \quad (2.4)$$

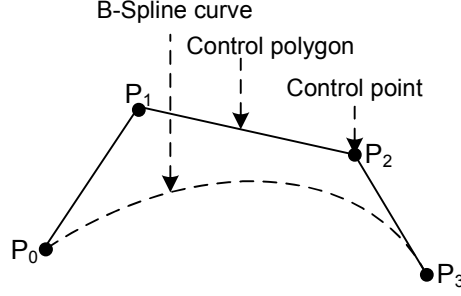


Figure 2.4: B-spline curve

where u is the independent variable and P_i is the control point. The polygon formed by P_i is called the control polygon as defined by Pourazaday and Xu (2000). $N_{i,p}(u)$ is the p -th degree B-spline basis functions defined as

$$N(u)_{i,0} = \begin{cases} 1 & u_i \leq u \leq u_{i+1} \\ 0 & \text{otherwise} \end{cases}, \quad (2.5)$$

$$N_{i,p}(u) = \frac{u - u_i}{u_{i+p} - u_i} N_{i,p-1}(u) + \frac{u_{i+p+1} - u}{u_{i+p+1} - u_{i+1}} N_{i+1,p-1}(u), \quad (2.6)$$

where it is defined over a non-periodic and non-uniform knot vector as

$$U = \left\{ \underbrace{0, \dots, 0}_{p+1}, u_{p+1}, \dots, u_{m-p-1}, \underbrace{1, \dots, 1}_{p+1} \right\}, \quad (2.7)$$

where p is the degree of basic function. Note that the number of knots is $m + 1$ and the number of control points is $n + 1$. Therefore, one has $m = n + p + 1$.

In what follows, the steps to determine the location of a point on a B-spline curve at a certain value u is itemized:

- Calculate the number of knots employing the number of control points and the degree of the function p .
- Define the coordinates of the B-spline control points.

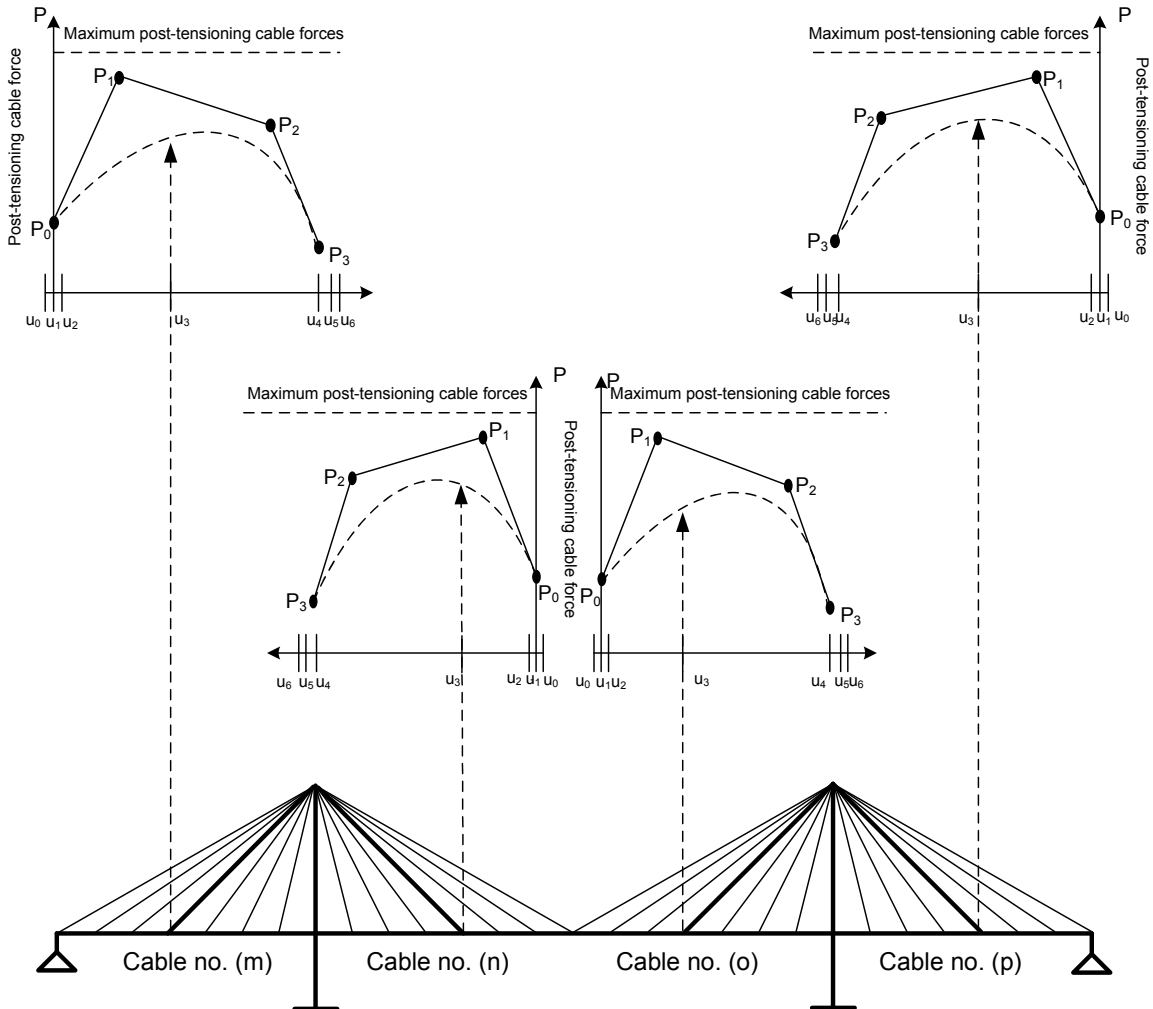


Figure 2.5: Representation of cable forces in a fan arrangement using B-spline curves.

- Calculate the non-zero basis functions as defined in Eq. (2.6).
- Multiply the values of the nonzero basis function with the corresponding control points.

2.3.3 Design Variables and Objective Function

The x and y -coordinates of the control points in B-spline curves are considered as the design variables denoted by P_i s in Fig. 2.5 and 2.6. These points define the shape of the B-spline curve representing the distribution of the post-tensioning cable forces, as depicted in Fig. 2.5 and Fig. 2.6. As shown, each highlighted cable is assigned to

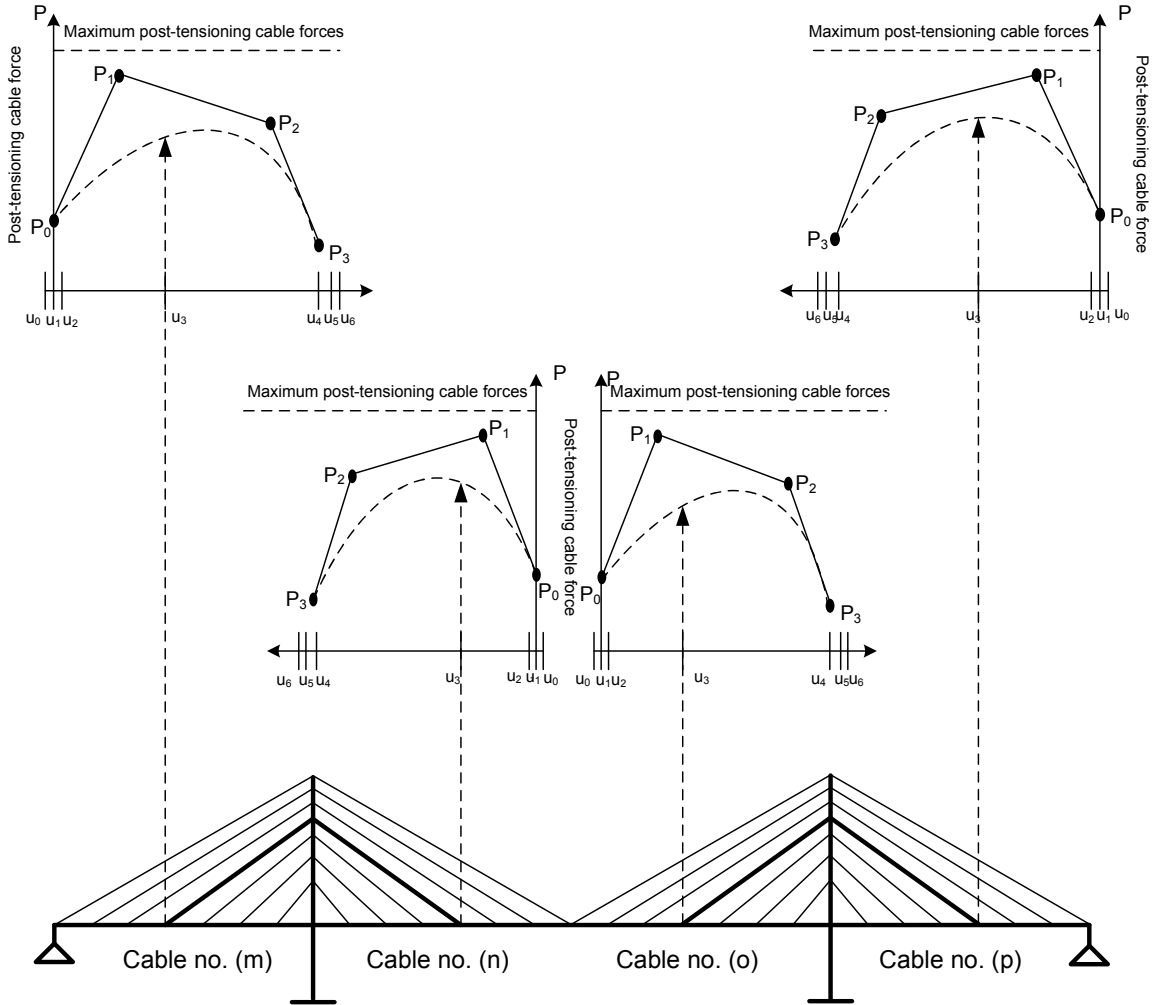


Figure 2.6: Representation of cable forces in a harp arrangement using B-spline curves.

a curve to determine their corresponding post-tensioning cable forces.

In Fig. 2.5, cable numbers i , j , k . and l are mapped to their respective post-tensioning cable forces value on the B-spline curves. Similar to the assumption employed by Hassan et al. (2012), the upper and lower bounds for the x -coordinates are the span length and zero, respectively, i.e., $(0 \leq x \leq \text{main span})$. The y -coordinate is upper bounded by a preset cable for the maximum cable tensile force and lower bounded by zero as, $(0 \leq y \leq T_{max})$.

For two arrangements of cable-stayed bridges, four B-spline curves are employed to model the post-tensioning functions as shown in Fig. 2.5 and 2.6 for fan, and harp

arrangements, respectively.

The square root of the sum of the squares (SRSS) of the vertical deflection of the nodal points of the deck and the squares of the lateral deflection of the top points of two pylons is applied as objective function and defined as

$$F = \sqrt{(\delta_{1d}^2 + \delta_{2d}^2 + \delta_{3d}^2 + \cdots + \delta_{kd})_{deck} + (\delta_{1p}^2 + \delta_{2p}^2 + \delta_{3p}^2 + \cdots + \delta_{kp})_{pylon}} \quad (2.8)$$

where δ_{id} , $1 < i < k$, is the vertical deflection of the nodes of the deck spine and δ_{ip} , $1 < i < k$ is the lateral deflections of the pylons' tops. Therefore, the constraint applies

$$\left| \frac{\delta_{dmax}}{M} \right| \leq \varepsilon, \quad (2.9)$$

where δ_{dmax} is the maximum vertical deflection of the deck, M is the length of the main span, and ε is a convergence tolerance and set to 10^{-4} . It is noted that the use of the SRSS improves the objective function as well. In addition, the applied constraint ensures that the ratio between the vertical deflection at any point of the deck and the length of the main span does exceed a small tolerance value ε .

2.3.4 Real Coded Genetic Algorithm

As mentioned in the previous sections, due to non-deterministic transition rules, operators, and multi-points search, a global optimization technique is required to obtain post-tensioning cable forces. Based on the theory of biological evolution and adaptation, the global optimization genetic algorithms are employed to perform many optimization problems (Gen and Cheng, 2000). Genetic algorithm has been employed to obtain the global optimization solutions for the post-tensioning cable forces of cable-stayed bridges by Hassan et al. (2012). The real coded genetic algorithm (RCGA) is a

Algorithm 2.1 Optimum Post-tensioning Cable Forces Algorithm

Inputs: population size, no. of generation, operators, LB and UB of the design variables

Outputs: post-tensioning cable forces with the smallest value of F function

1. Develop the finite element model for the cable-stayed bridge
 2. Generate an initial population of the B-spline curves and compute the post-tensioning forces
 3. Apply the post-tensioning cable forces with dead load to the FEM.
 - 3.1 Calculate the deck and pylon deflections
 - 3.2 Evaluate the objective function F (given in Eq. (2.8)) value
 4. Sort the population in an ascending order to the value of the objective function F
 5. if $|\frac{\delta_{dmax}}{M}| \leq \varepsilon$ then
 - 5.1 Deliver the post-tensioning cable-forces with the smallest value of F
 - 5.2 else
 - 5.2.1 Generate a new population of the B-spline curves from GAs
 - 5.2.2 Replace the previous population with the new population and go to Step 3
 6. end if
 7. Return the post-tensioning cable-forces with the smallest value of F
-

variant of Genetic algorithm that is suitable for the optimization of multiple-optima objective functions defined over continuous variables. This algorithm operates directly on the design variables, instead of encoding them into binary strings in the traditional genetic algorithms. The genetic algorithm is used to select the lower and upper bounds of each design variables. The main purpose of the RCGA is to optimize the shapes of the post-tensioning functions to achieve minimum deflections, i.e., vertical deflection of the deck and lateral deflection of the pylons.

2.3.4.1 Genetic Operators

In the previous work by Hassan et al. (2012), boundary mutation, non-uniform mutation, and uniform mutation are used. The first operator searches the boundaries of the independent variables, the second is random search that decreases its random movements with the progress of the search, and the third is a totally random search element. The crossover operators produce new solutions from parent solutions having good objective function values (El Ansary et al., 2010).

In the current study, this translates into producing new post-tensioning function from pairs of post-tensioning functions. The crossover operators used are the arithmetic, uniform and heuristic crossovers. The first produces new solutions in the functional landscape of the parent solutions. The second one is used to create a new solution randomly from two parents, while the last one extrapolates the parent solutions into a promising direction (Hassan et al., 2012).

2.3.5 Optimum Post-tensioning Cable Forces Algorithm

The algorithm which combines the finite element model, B-spline function, and real coded genetic algorithm (RCGA) for finding the optimum post-tensioning cable forces distribution under dead load is given in Algorithm 2.1. As one can see, first, three dimensional finite element models for three arrangements of cable-stayed bridges are developed. Then, an initial population of the design variables (the coordinates of B-spline control points) are randomly selected using genetic algorithm. The search points in the population is used to create a candidate function for each arrangement. The post-tensioning forces is obtained using the post-tensioning function and are applied to the finite element model to obtain the objective functions. The initial population should be sorted in such a way that the first ranked candidate has the minimum F function value. Next, genetic algorithm is employed again to generate new population on the high ranked post-tensioning function. This procedure should

be performed iteratively as shown in Algorithm 2.1 to obtain the candidate post-tensioning function.

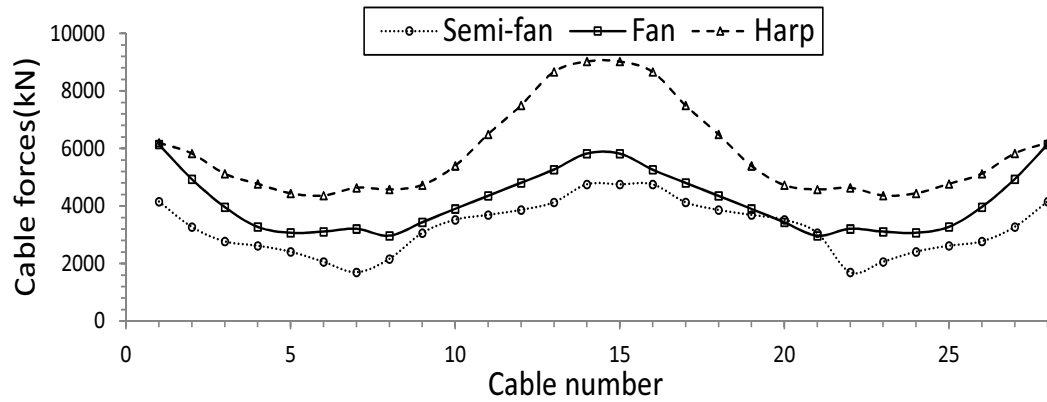
In the following section, the Algorithm 2.1 is employed to obtain the post-tensioning cable forces for three arrangements of cable-stayed bridges.

2.4 Post-tensioning Cable Forces for Three Cable Arrangements of Cable-Stayed Bridges

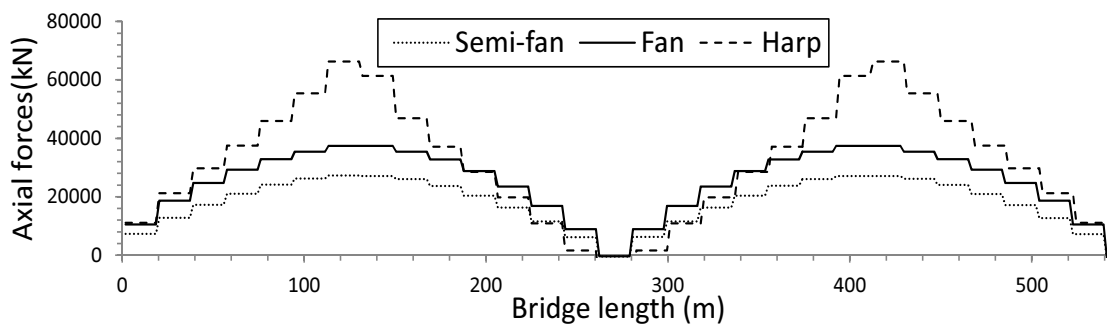
In this section, the results of post-tensioning cable forces are provided for three arrangements of cable-stayed bridges using Algorithm 2.1. The effect of the variation of mid-span length (M) and upper strut height (h) on the post-tensioning cable forces is investigated. Also, the results under the distribution of dead load for three arrangements, i.e., fan, semi-fan and harp cable-stayed bridges are compared to each other.

2.4.1 Post-tensioning Cable Forces for Three Cable Arrangements of Quincy Bayview Bridge

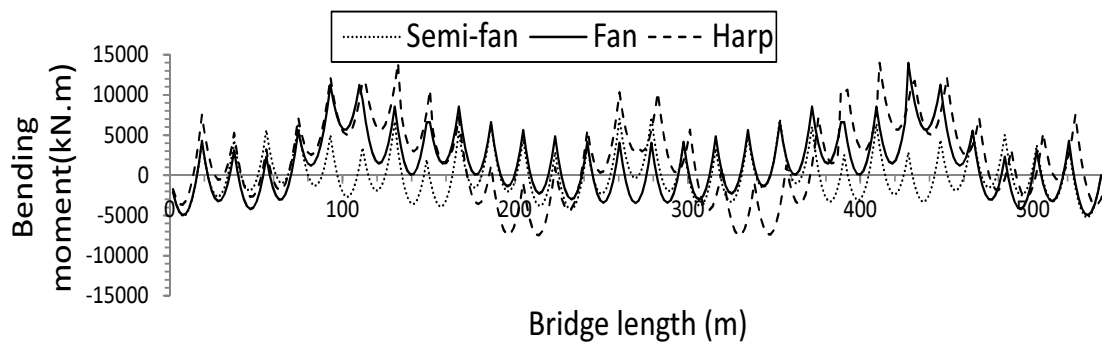
In this section, the results of post-tensioning cable forces are provided for three arrangements of Quincy Bayview bridge, i.e., fan, semi-fan and harp using Algorithm 2.1. Also, the distribution of the axial forces and bending moment on the deck are illustrated. As it is described in the previous sections, the bridge configurations are: the number of stay cables (in each group) $n = 7$, height of the pylon $h = 45$, mid-span length $M = 285.8$, and bridge length $L = 542$ m. The results indicate that the values of post-tensioning cable forces for the harp arrangement are higher than the values for fan and semi-fan arrangements as illustrated in Fig. 2.7a. Note that the semi-fan arrangement has the least post-tensioning forces and the fan arrangement lies in



(a) Post-tensioning cable forces.



(b) Axial forces of the deck



(c) Bending moment of the deck.

Figure 2.7: Distribution of cable forces in Bayview Bridge

between them. As one can see in Fig. 2.7a, the distribution of the post-tensioning cable forces are more uniform. The maximum post-tensioning cable forces for the harp arrangement is about 8,800 kN which reduces to 6,000 kN for the fan layout. The maximum cable forces for the semi-fan arrangement is about 5,200 kN which is close to the post-tensioning cable forces of the fan arrangement. In Fig. 2.7b, the axial forces on the deck are illustrated. As one can see, the harp arrangement has larger axial forces in comparison to the fan and semi-fan arrangements. Note that the semi-fan arrangement has the least axial forces and the fan arrangement lies in between them. The maximum axial forces on the deck for the harp arrangement is 6,400 kN which is higher than the maximum axial forces for the fan and semi-fan arrangement. The distribution of the axial forces on the deck are more uniform for the fan and semi-fan arrangement. The maximum axial forces for the fan arrangement is 3,800 kN which is close to the maximum axial forces for the semi-fan arrangement (3,400 kN). Also, in Fig. 2.7c, the distribution of the bending moment of the deck is plotted in terms of bridge length for three arrangements. It should be noted that, the distribution of bending moment of the deck for the semi-fan arrangement is more uniform in comparison to the harp and fan arrangement. One can see that, the harp type has the maximum bending moment of the deck, which is 13,000 $kN.m$. The maximum bending moment for the semi-fan layout is 6,000 $kN.m$ and it is close to the fan type (8,000 $kN.m$). In Fig. 2.8 the bending moments of the pylon is plotted in terms of pylon height for three arrangements. The bending moments of the pylon bottom are 13,420 $kN.m$, 9,853 $kN.m$, and 5,935 $kN.m$ for semi-fan, fan, and harp arrangements, respectively, as shown in Fig. 2.8.

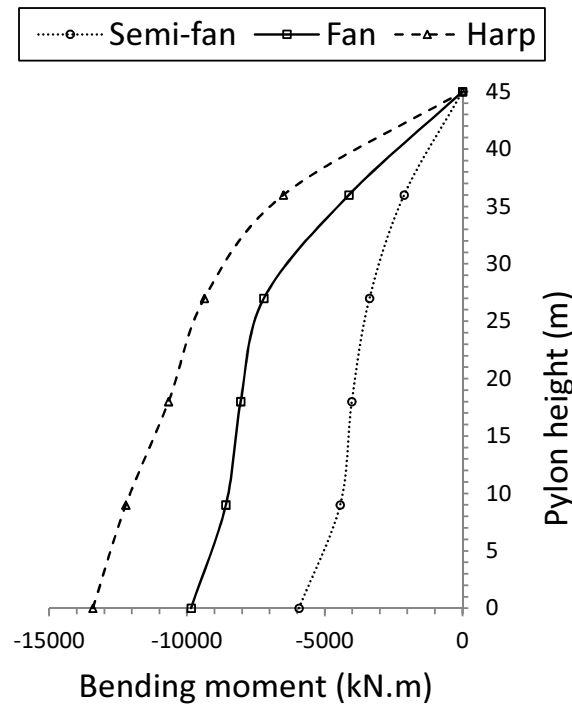


Figure 2.8: Bending moment of the pylon in Bayview Bridge.

2.4.2 The Effect of Height of the Pylon on the Distribution of Post-tensioning Cable Forces with $n = 7$, $h = \{20, 40, 60\}$, and $M = 260$

In this section, the variation of the pylon height on the distribution of post-tensioning cable forces is investigated. As shown in Fig. 2.9, the post-tensioning cable forces for the three different arrangements of cable-stayed bridges are illustrated while keeping the number of cables and mid-span length unchanged. Three different values $h = 20$ m, 40 m, and 60 m are considered for the upper strut height. The result shows that the values of post-tensioning cable forces for the harp style are typically higher than the fan and semi-fan values. The semi-fan arrangement has the least post-tensioning forces and the fan style lies in between them. It is clear that as the height of the pylon increases, the resultant forces (compressed by pylon) decreases and consequently the

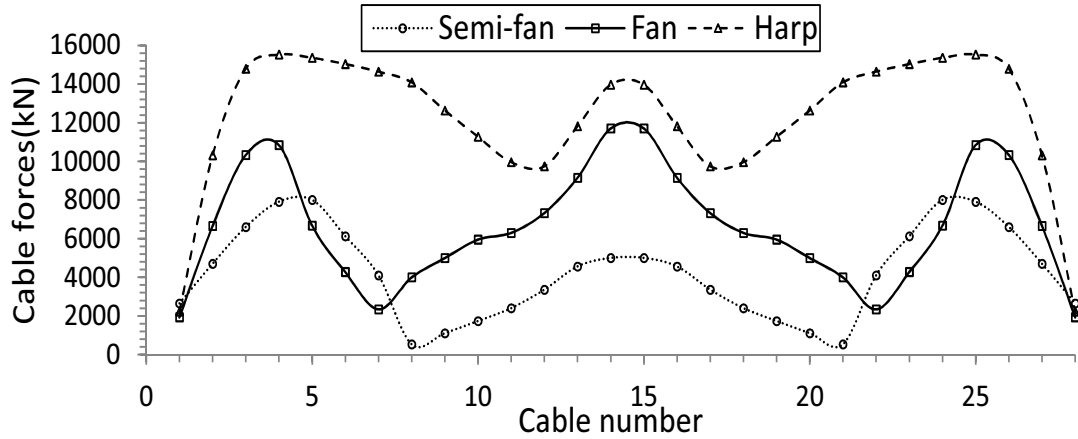
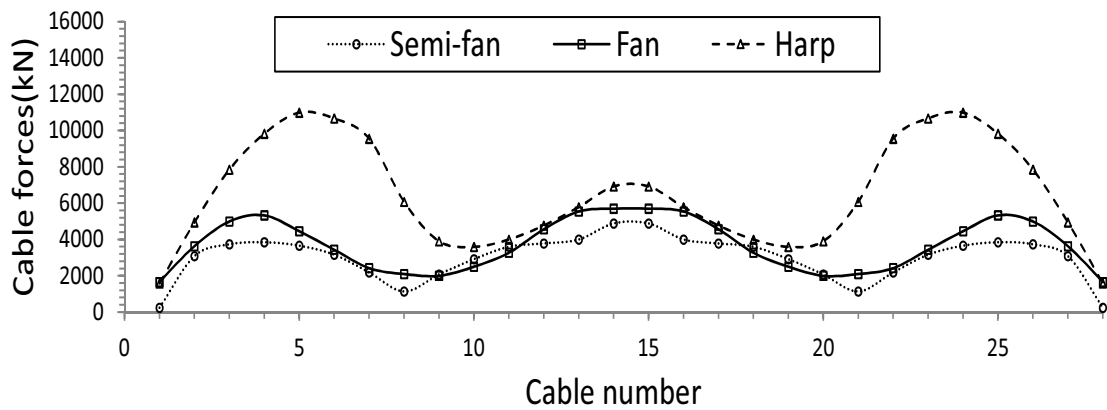
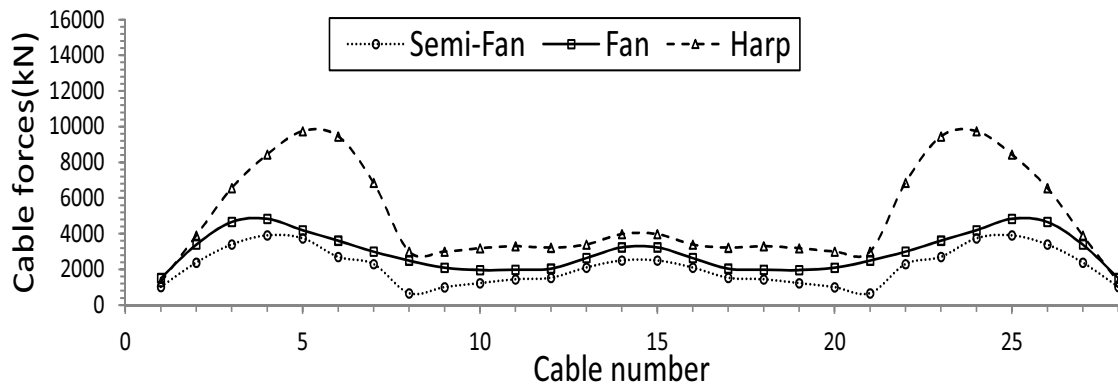
(a) $n = 7$, $M = 260$ m, and $h = 20$ m(b) $n = 7$, $M = 260$ m, and $h = 40$ m(c) $n = 7$, $M = 260$ m, and $h = 60$ m

Figure 2.9: The post-tensioning stay cable forces for three main types of cable-stayed bridges with constant number of cables ($n = 7$), constant mid-span length ($M = 260$) and variable upper strut height ($h = 20, 40, 60$).

post-tensioning cable forces decrease. For instance, as one can see in Figs. 2.9a, 2.9b, and 2.9c, the maximum post-tensioning cable forces for $h = 20$ m is about 16,000 kN which reduces to 10,000 kN with $h = 60$ m. It is worth mentioning that the decrease in post-tensioning cable forces for semi-fan and harp is considerable in comparison to the fan arrangement. The distribution of the post-tensioning cable forces are more uniform when the pylon height is 60 m. The results indicate in general that, variation of height of the pylon has a significant effect on the post-tensioning cable forces.

2.4.3 The Effect of Mid-span Length on the Distribution of Post-tensioning Cable Forces with $n = 7$, $h = 20$, and $M = \{260, 270, 280\}$

In this section, the effect of variation of mid-span length on the post-tensioning cable forces is investigated. The mid-span length is increased from $M = 260$ m to $M = 280$ m while keeping the number of stay cables and the pylon height unchanged. The results are illustrated in Fig. 2.10. The effect of increasing the mid-span length, M on the post-tensioning cable forces is assessed for these three mid-span values. The results indicate that the post-tensioning cable forces increase as the mid-span length increases. The comparisons in Figs. 2.10a, 2.10b, and 2.10c, indicates that the longer span-length has larger post-tensioning cable forces. The post-tensioning cable forces of the outer cables (longest cables) for all three arrangements increases rapidly with the increase in the mid-span length. In all cases, the harp arrangement has higher post-tensioning cable forces in comparison to the other arrangements.

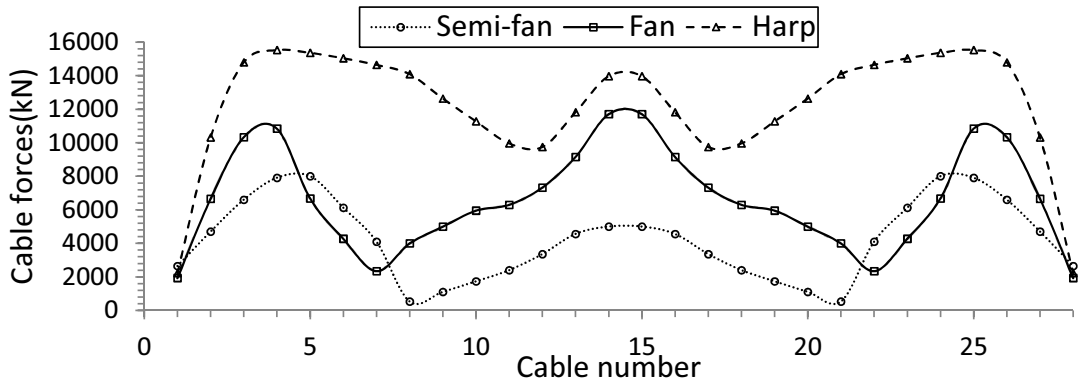
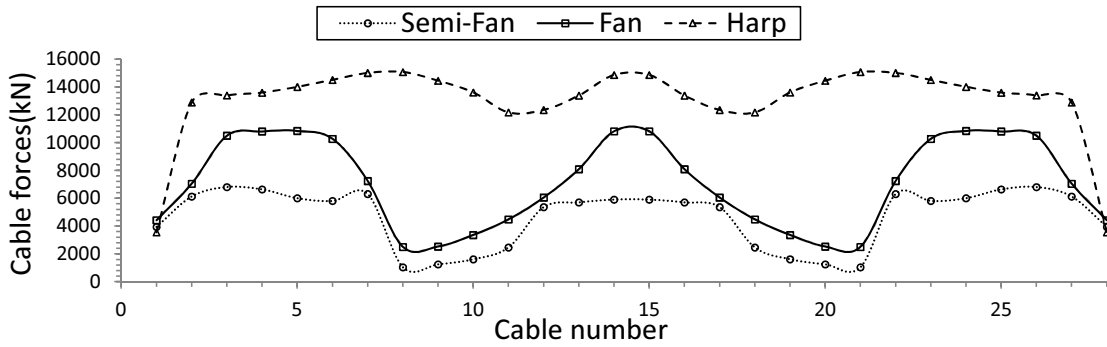
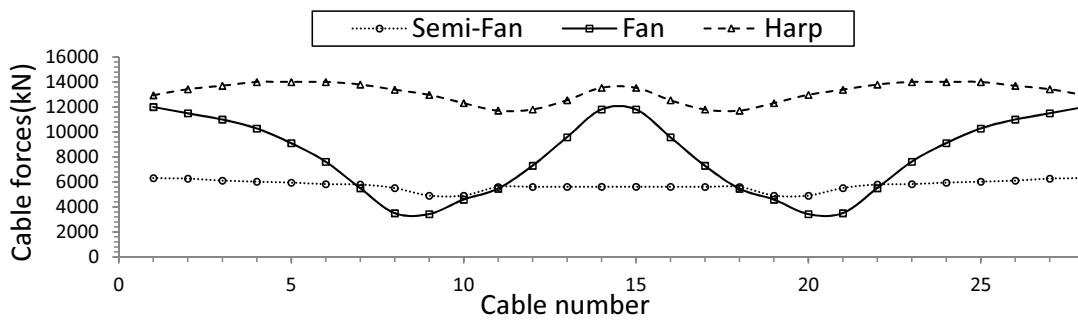
(a) $n = 7$, $M = 260$ m, and $h = 20$ m(b) $n = 7$, $M = 270$ m, and $h = 20$ m(c) $n = 7$, $M = 280$ m, and $h = 20$ m

Figure 2.10: The post-tensioning stay cable forces for three main types of cable-stayed bridges with constant number of cables ($n = 7$), constant mid-span length ($M = 260, 270, 280$ m) and variable upper strut height ($h = 20$).

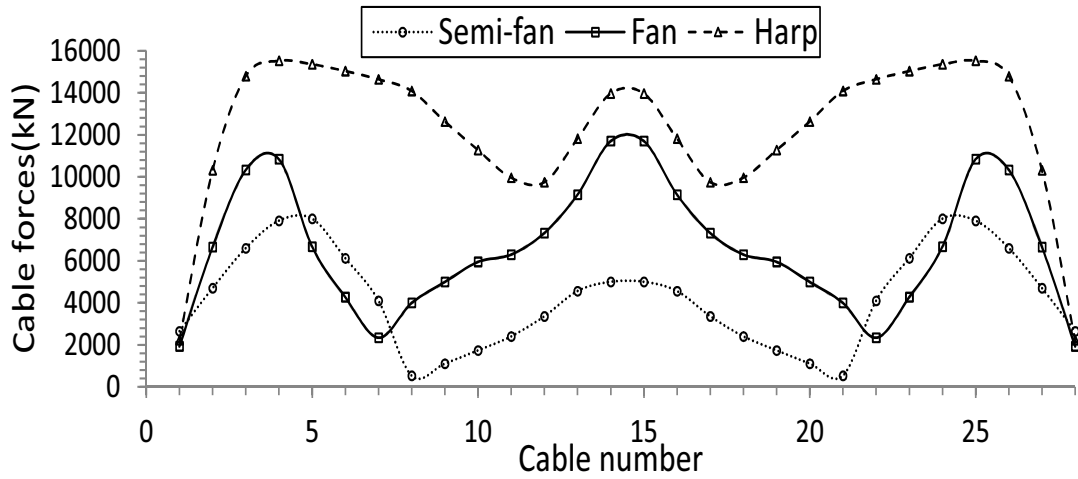
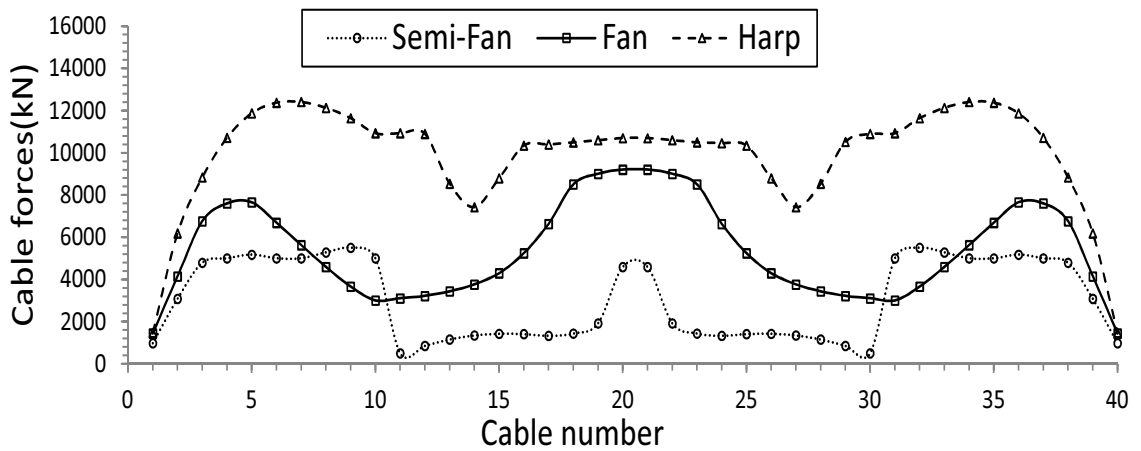
(a) $n = 7$, $M = 260$ m, and $h = 20$ m(b) $n = 10$, $M = 260$ m, and $h = 20$ m

Figure 2.11: The post-tensioning stay cable forces for three main types of cable-stayed bridges with variable number of cables ($n = 7, 10$), constant mid-span length ($M = 260$ m), and constant height of the pylon ($h = 20$ m).

2.4.4 The Effect of Number of Cables on the Distribution of Post-tensioning Cable Forces with $n = \{7, 10\}$, $h = \{20\}$, and $M = \{260\}$.

In this subsection, the effect of increasing the number of stay cables for the three different arrangements of cable-stayed bridges is assessed. The post-tensioning cable forces for different values of n , are determined while keeping the height of the pylon h , and the mid-span length M , unchanged.

Increasing the number of cables distributes the effect of dead load of the deck to the cables and hence the post-tensioning cables forces will be reduced. As one compares Fig. 2.11a and Fig. 2.11b the cable forces reduced when the number of cables increased from $n = 7$ to $n = 10$.

In the fan style, increasing the number of the stay cables increases the anchorages weights, and makes them very difficult to attach to the top of the pylon. For the harp arrangement, increasing the number of stay cables requires to increase the pylon height to make it possible to accommodate extra cables.

In this study, as shown in Fig. 2.11, the number of stay cables is increased from 7 to 10 and the height of the pylon and mid-span length are kept unchanged. As one can see, for all three arrangements, as the number of cables increases, the post-tensioning cable forces reduce. It is worth mentioning that, in comparison to the cases with $n = 7$, the post-tensioning cable forces for the case $n = 10$ (Fig. 2.11b) are reduced and are uniformly distributed amongst all of the cables.

As illustrated in Fig. 2.11b, semi-fan arrangement has the lowest post-tensioning cable forces in comparison to the two other arrangements. The harp arrangement has the highest post-tensioning cable forces in all of its cables. The fan arrangement lies between other two arrangements. It should be noted that in some cases for the outer cables (longest cables), the post-tensioning cable forces for fan arrangement is

slightly less than the semi-fan arrangement.

2.5 Conclusion

In this chapter, the effect of three main parameters of the cable stayed-bridges on post-tensioning cable forces is studied. First, the method proposed by Hassan et al. (2012) is employed in this study to obtain the post-tensioning cable forces for three main arrangements of cable-stayed bridges, i.e., semi-fan, fan, and harp. Then, the effect of increasing the pylon height, mid-span length, and the number of stay cables on the post-tensioning cable forces are investigated. Moreover, the determined post-tensioning cable forces for fan, semi, fan, and harp arrangements are compared with each other. The results indicates that the semi-fan style has the least post-tensioning cable forces and harp arrangement has the largest post-tensioning forces in all of the cables. It is further noted that increasing the number of stay cables reduces the post-tensioning cable forces. However, this should be handled very carefully for the fan arrangement due to the limited space to accommodate more cables at the top of the pylon. The conclusions that can be drawn from this chapter are numerated as follows:

- The variation of height of the pylon has a significant effect on the post-tensioning cable forces. The effect of increasing the pylon height on the post-tensioning cable forces is more visible in the inner stay cables harp arrangements.
- The post-tensioning cable forces increase as the mind-span length increases. Also, the post-tensioning cable force of the outer cables (longest cables) increases rapidly with the increase of the main span length.
- Increasing the number of cables distributes the effect of dead load of the deck to the cables and hence the post-tensioning cables forces are reduced.

- Amongst three arrangements of cable-stayed bridges, the harp arrangements has the highest post-tensioning cable forces in all of its cables. The semi-fan arrangement has the lowest post-tensioning cable forces and the fan arrangement lies between them.

Bibliography

- M. Hassan. *Optimum Design of Cable-Stayed Bridges*. PhD thesis, The University of Western Ontario, 2010.
- John. Wilson and Wayne Gravelle. Modelling of A Cable-Stayed Bridge For Dynamic Analysis. *Journal of Earthquake Engineering and Structural Dynamics*, 20:707–771, 1991.
- M.M. Hassan, A. A. El Damatty, and Nassef. Determination of Optimum Post-Tensioning Cable Forces for Cable-stayed Bridges. *Journal of Engineering Structures*, in press, 2012.
- H. Bernard, Isler Walmer, and Moia Pierre, editors. *Cable Stayed Bridges*. Presses Polytechniques Romandes, Lausanne, Switzerland, 1988. ISBN 0-7277-1321-3.
- K. Tori, K. Ikeda, and T Nagasaki. A Non-iterative Optimum Design Method for Cable-Stayed Bridges. In *Proceedings of Japan Society of Civil Engineers*, pages 115–123, 1968.
- LMC. Simoes and JHJO Negroao. Sizing and Geometry Optimization of Cable-stayed Bridges. *Journal of Computer and Structure*, 52:309–321, 1994.
- W.X. Ren and X.L. Peng. Baseline finite element modeling of a large span cable-stayed bridge through field ambient vibration tests. *Computers & structures*, 83(8):536–550, 2005.

- F. Nieto, S. Hernandez, and J A. Julardo. Optimum Design of Long-span Suspension Bridges Considering Aeroelastic and Kinematic Constraints. *Journal of Structure Multidisc. Optim.*, 39:133–151, 2009.
- W. Long, MS. Troitsky, and ZA Zielinski. Optimum Design of Cable Stayed Bridges. *Journal of Structural Engineering and Mechanics*, 7:241–257, 1999.
- LMC. Simoes and JHJO Negro. Optimization of Cable-Stayed Bridges with Box-girder Decks. *Journal of Advanced Engineering*, 31:417–423, 2000.
- D. Jajnic, M. Pircher, and H Pircher. Optimization of Cable Tensioning in Cable-Stayed Bridges. *Journal of Bridge Engineering*, 8:131–137, 2003.
- YU-CHi. Sung, Dyi-Wei. Chang, and Eng-Huat Teo. Optimum Post-Tensioning cable Forces of Manu-Lo Hsi Cable-Stayed Bridge. *Journal of Engineering Structures*, 28:1407–1417, 2006.
- T.Y. Lee, Y.H. Kim, and S.W. Kang. Optimization of tensioning strategy for asymmetric cable-stayed bridge and its effect on construction process. *Structural and Multidisciplinary Optimization*, 35(6):623–629, 2008.
- V. Lute, A. Upadhyay, and KK Singh. Computationally Efficient Analysis of Cable-stayed Bridges for GA-based Optimization. *Journal of Engineering Applied Artificial Intell.*, 22(4-5):750–758, 2009.
- A. Baldomir, S. Henandez, F. Nieto, and A Jurado. Cable Optimization of a Long Span Cable-Stayed Bridge in La Coura (Spain). *Journal of Advances in Engineering Software*, 41:931–938, 2010.
- Tao. Zhang and ZhiMin Wu. Dead Load Analysis of Cable-Stayed Bridge. In *International Conference on Intelligent Building and Management (CSIT'11)*, pages 270–274, 2011.

- PH. Wang, TC. Tseng, and CG Yang. Initial Shape of Cable Stayed Bridges. *Journal of Computational Structure*, (46):1095–1106, 1993.
- JH Ernst. Der E-Modul von Seilen unter berucksichtigung des Durchhanges. *Der Bauingenieur*, 40(2):52–59, 1965.
- AS. Nazmy and AM. Abdel-Ghaffar. Three-dimensional nonlinear static analysis of cable-stayed bridges. *Journal of Structural Engineering*, 34(2):257–271, 1990.
- W Jr Weaver and JM Gere, editors. *Matrix Analysis of Framed Structures*. 3rd Edn, New York: Van Nostrand Reinhold; 1980, 1980.
- M. Gen and R. Cheng, editors. *Genetic Algorithms and Engineering Optimization*. Wiley, NewYork, 2000. ISBN 0-7277-1321-3.
- M. Pourazaday and X. Xu. Direct Manipulations of B-spline and NURBS Curves. *Journal of Advances in Engineering Software*, 31(2):107–118, 2000.
- AM El Ansary, AA El Damatty, and AO Nassef. A coupled finite element genetic algorithm technique for optimum design of steel conical tanks. *Thin-Walled Structures*, 48(3):260–273, 2010.
- CAN/CSA-S6-06. Canadian highway bridge design code s6-06 (can/csa s6-06). *Canada: Canadian Standard Association, Ontario*, 2006.
- AASHTO.LRFD. Bridge Design Specifications. *4th Edition Washington D.C., USA*, 2007.
- L Davis, editor. *Handbook of Genetic Algorithms*. Van Nostrand Reinhold, New York, USA, 1991. ISBN 0-7277-1321-3.
- Z Michalewics and DB Fogel, editors. *How to Solve it: Modern Heuristics*. 2nd Edition, Springer, New York, USA, 2004.

R Walther, B Houriet, W Isler, P Moia, and JF Klein. Cable-Stayed Bridges. *Thomas Telford Ltd*, 1988.

MS Troitsky, editor. *Cable-Stayed Bridges: Theory and Design*. 2nd Edition, Oxford: BSP 1988, 1988.

Chapter 3

Optimal Design of Harp, Fan, and Semi Fan Cable-Stayed Bridges

IN the recent decade, considerable research has been conducted on the optimum design of cable-stayed bridges, which are considered as the most suitable structure system for medium to long span bridges with span length ranging from 200 to about 1000 meter. This is due to their aesthetic, economic, and the ease of erection. Achieving the optimum design for cable-stayed bridges is a challenging task. This is due to the fact that the design is influenced by a large number of variables, including geometrical configurations, number of stay cables, types of pylons, arrangement of the stay cables, and the types of main girder. As mentioned in the previous chapter, stay cables of a cable-stayed bridge are typically post-tensioned to counter balance the effect of dead load on the deck and pylon. These cable forces affect directly the performance and the economic efficiency of cable-stayed bridges. An entropy-based optimization algorithm to optimize the cost of cable-stayed bridges was proposed by Simoes and Negrao (1994). The locations of stay cable along the main girder and pylon, and the cross-sectional sizes of the deck, pylons, and stay cables were considered as the design variables. In their work, the number of stay cables and the mid-span

length were assumed as preassigned constant parameters. Long et al. (1999) used an internal penalty function algorithm to optimize the cost of cable-stayed bridges with composite superstructure. The bridge is modeled as a 2-D structure while including the geometric non-linear effect. The design variables included the parameters that describe the cross sectional dimensions of the bridge elements. The height of pylon, the mid-span length, and the number of stay cables are kept constant with preassigned values. It should be noted that the effect of the post-tensioning cable forces was not considered in their study (Long et al., 1999). Simoes and Negrao (2000) proposed a function called convex scalar function, which is used to optimize the cost of the deck in cable-stayed bridges. Convex scalar function combines dimensions of the cross-sections of the bridge and post-tensioning cable forces. The design variables included maximum allowable stresses, minimum stresses in the stay cables, and deflections of the deck. Note that the pylon height and the mid-span length were not considered by Simoes and Negrao (2000). Recently, Lute et al. (2009) has proposed a genetic algorithm (GA) which was employed to reduce the computational time of optimizing cable-stayed bridges. It was indicated that the genetic algorithm is an efficient tool for solving cable-stayed bridge optimization problems. The number of stay cables was treated as a pre-set design variable, and the effect of post-tensioning cable forces was not considered in their study.

Most recently, optimal design of cable-stayed bridges has been considered by Baldomir et al. (2010), Hassan et al. (2012), and Lee et al. (2008) available in the literature. In Chapter 2, the effect of varying pylon height, mid-span length, and number of cables on the post-tensioning cable forces for fan, semi-fan, and harp arrangements has been investigated and compared with each other. The objectives of this chapter are to conduct a study to determine the optimum design cost of the three main types of cable-stayed bridges, compare between those costs, and assess the effect of various parameters on the optimum cost value.

To date, this is the first comprehensive cost evaluation of three main arrangements of cable-stayed bridges that considers all components of cable-stayed bridges, i.e., pylon height, mid-span length, and the number of stay cables.

3.0.1 Design Variables

The optimum cost design of cable-stayed bridges has several design parameters. The vector of design variables $\{x\}$ includes the number of stay cables, geometric configuration, and cross-sectional dimensions of bridge elements. These design variables are selected based on the designer experiences. More specifically, the vector of design variables $\{x\}$ can be written as follows:

$$\{x\} = \{N, \gamma_1, \gamma_2, \gamma_3, \gamma_4, D, t_s, H_G, F_{FT}, F_{FB}, F_{wl}, H_P, B_P, t_p\}, \quad (3.1)$$

where

- N is the number of stay cables in each single plane as shown in Fig. 3.1.
- $\gamma_1 = \frac{M}{L}$, M is the mid-span length and L is the total length of the bridge, shown in Fig. 3.1.
- $\gamma_2 = \frac{h_B}{L}$, h_B is the height of the upper strut beam as shown in Figs. 3.3a and 3.3b.
- D is the diameter of a stay cable.
- t_s is the thickness of the concrete deck slab as shown in Fig. 3.2a.
- H_G is the height of the two steel main girders, shown in Fig. 3.2b.
- $\gamma_3 = \frac{B_{FT}}{H_G}$, B_{FT} is the width of the top flange as shown in Fig. 3.2b.
- $\gamma_4 = \frac{B_{FB}}{H_G}$, B_{FB} is the width of the bottom flange as shown in Fig. 3.2b.

- F_{FT} , is a factor defining the thickness of the upper flange. In CAN/CSA-S6-06 (2006), a range of values for “ F_{FT} ” are given in order to prevent premature local buckling of the flange. Thickness of the upper flange, shown in Fig. 3.2b, is calculated as:

$$t_{FT} = \frac{B_{FT}\sqrt{F_y}}{2F_{FT}} \quad (3.2)$$

where B_{FT} is the width of upper flange, F_y is steel yield strength, and F_{FT} is the factor decides the thickness of top flange.

- F_{FB} is the factor defining the thickness of the bottom flange. Based on the range of values of the F_{FB} given in CAN/CSA-S6-06 (2006), the thickness of the bottom flange, shown in Fig. 3.2b, is calculated using:

$$t_{FB} = \frac{B_{FB}\sqrt{F_y}}{2F_{FB}} \quad (3.3)$$

where B_{FB} is width of the bottom flange, F_y is steel yield strength, and F_{FB} is a factor that decides the thickness of the lower flange.

- F_{w1} is the factor defining the thickness of the web in order to prevent premature local buckling. The thickness of the web, shown in Fig. 3.2b, is calculated in CAN/CSA-S6-06 (2006) as:

$$t_w = \frac{H_G}{\left(\frac{F_{W1}}{\sqrt{F_y}} \left[1 - F_{W2} \frac{F_{fw}}{F_{yw}} \right] \right)} \quad (3.4)$$

where F_{fw} is factor defining compressive force in the web component at ultimate limit state, F_{yw} is axial compressive force at yield stress, F_{W2} is 0.39, 0.61, and 0.65 for Class 1, 2 and 3, respectively, as given in CAN/CSA-S6-06 (2006).

- H_P , B_P , and t_p , are the depth, width, and thickness of the pylon cross-section as shown in Fig. 3.3c.

Table 3.1: Three factors define thickness of steel main girders [Clause 10.9.2 ,CAN/CSA-S6-2006]

	Class 1	Class 2	Class 3
Upper flange	$F_{FT} \leq 145$	$145 \leq F_{FT} \leq 170$	$170 \leq F_{FT} \leq 200$
Lower flange	$F_{FB} \leq 145$	$145 \leq F_{FB} \leq 170$	$170 \leq F_{FB} \leq 200$
Web	$F_{W1} \leq 1100$	$1100 \leq F_{W1} \leq 1700$	$1700 \leq F_{W1} \leq 1900$

Table 3.2: Lower and upper bounds of the design variables

Design variable	Definition	Lower bound	Upper bound
N	Number of stay cable in each single plane	5	14
γ_1	mid-span length / bridge length	0.48	0.54
γ_2	height of upper strut cross beam/bridge length	0.03	0.11
D	Diameter of each stay cable	0.01 m	0.15 m
t_s	Thickness of concrete deck slab	0.15 m	0.23 m
H_G	Height of the two steel main girders	1 m	5.0 m
γ_3	width of top flange/height of main girder	0.15	0.20
γ_4	width of bottom flange/height of main girder	0.20	0.15
F_{FT}	Factor decides the thickness of upper flange	145	200
F_{FB}	Factor decides the thickness of lower flange	145	200
F_{w1}	Factor decides the thickness of web	1100	1900
H_P	Depth of the pylon cross-section	1.0 m	5.0 m
B_P	Width of the pylon cross-section	1.0 m	5.0 m
t_p	Thickness of the pylon cross-section	0.5 m	1.0 m

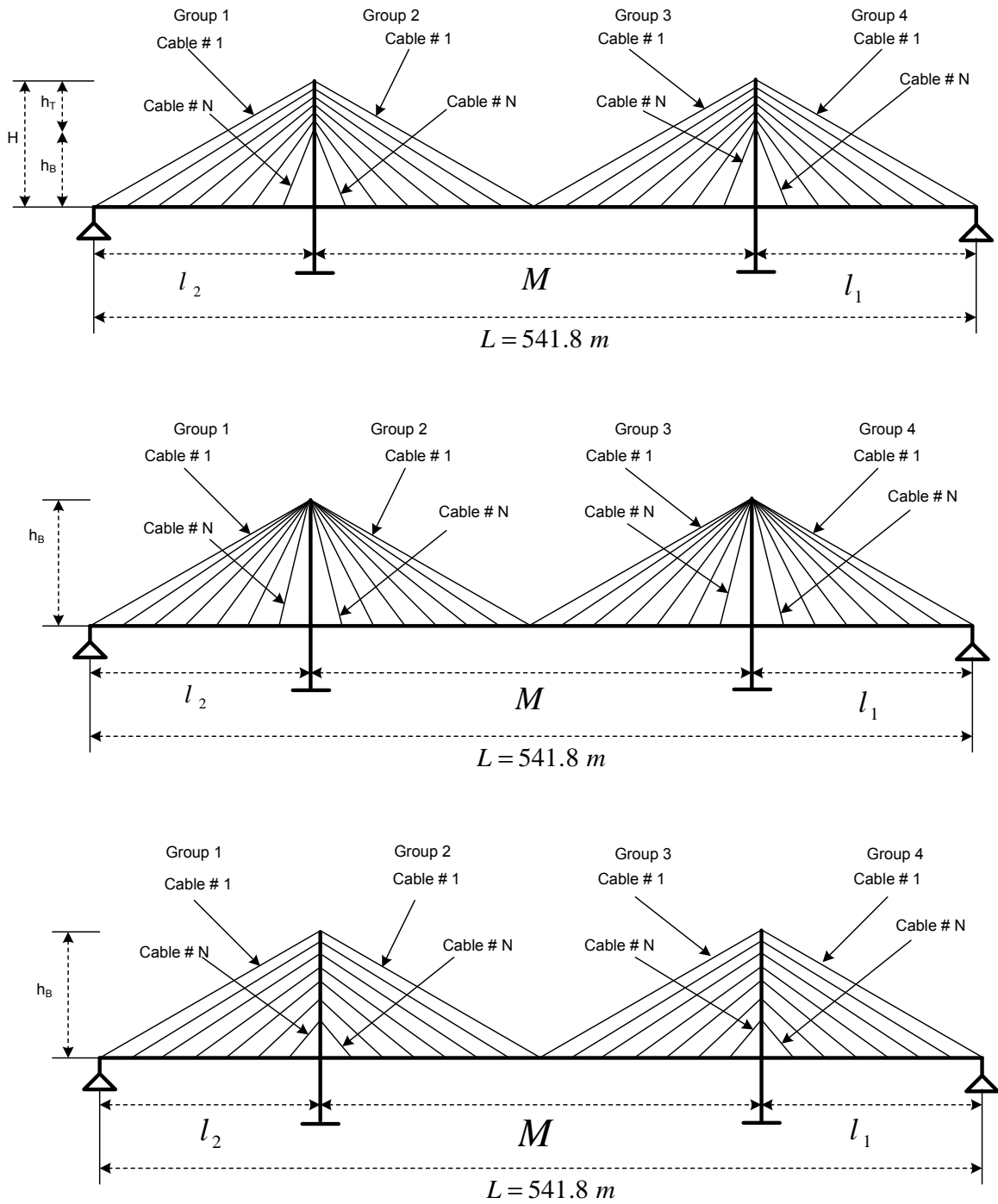


Figure 3.1: Geometry of three arrangement of cable-stayed bridges

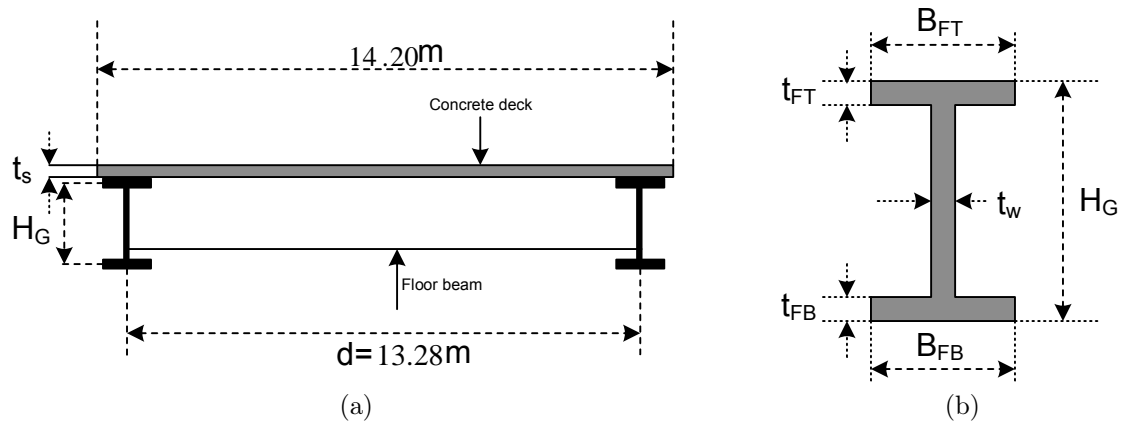


Figure 3.2: Bridge deck cross section (a) Cross-section of the bridge deck for three arrangement of cable-stayed bridges and (b) Steel main girder.

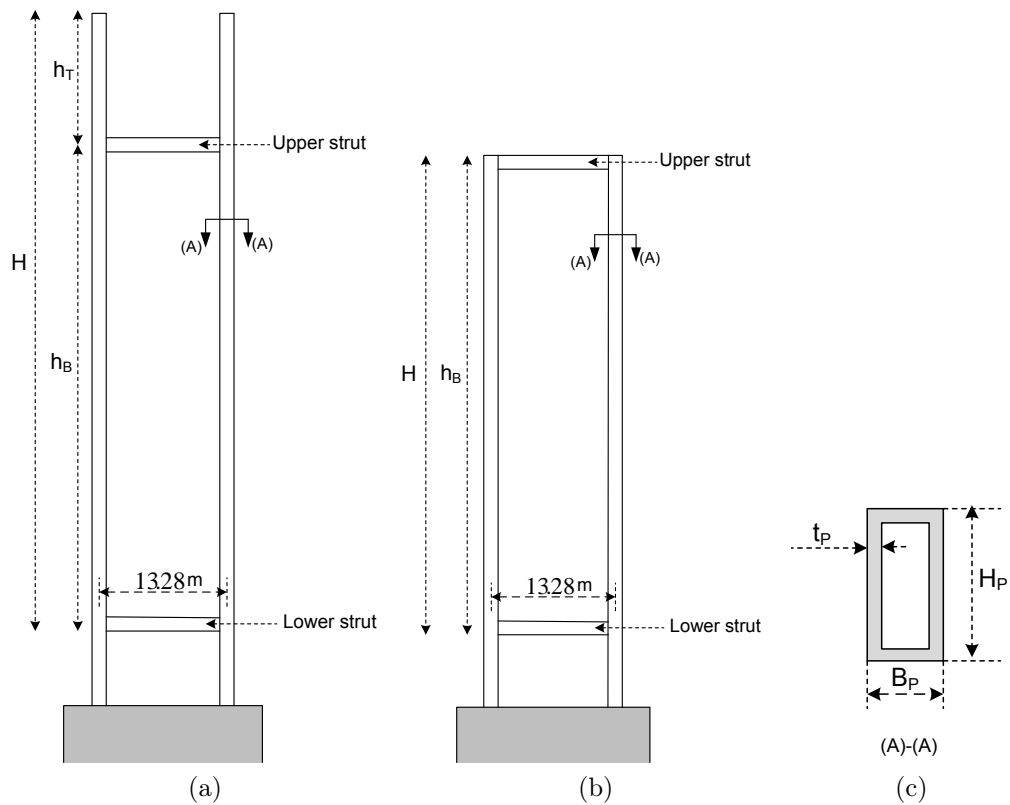


Figure 3.3: Pylon elevation of three arrangement of cable-stayed bridges (a) Pylon elevation for semi-fan (b) Pylon elevation for harp and fan (c) Pylon cross-section.

The range of all these three factors depends on the different class of the cross section and is provided in Table 3.1 based on CAN/CSA-S6-06 (2006).

The upper bounds and lower bounds of these eleven design variables are all included in Table 3.2.

3.0.2 Design Constraints

The design of cable-stayed bridges requires checking stresses in the stay cables, the deck girders, and the pylons due to dead, live, and wind loads acting on the bridge. The design constraints functions are determined based on the provision provided in Canadian Highway Bridge Design Code CAN/CSA-S6-06 (2006) and are included in the numerical code. The constraint functions g_i for each components of cable stayed bridge are provided below:

3.0.2.1 Stay cables

The stay cables resist only tensile forces. As such, the following conditions has to be satisfied:

$$g_1 = T_{fcable} - 0.55T_{ucable} \leq 0 \quad (3.5)$$

$$T_{ucable} = \frac{(\pi D^2)}{4} T_{cCable} \quad (3.6)$$

where T_{fcable} , is the factored tensile force in the stay cable, T_{ucable} , is the specified minimum tensile resistance, D is the diameter of the stay cable and T_{cCable} , is ultimate tensile strength of the stay cable.

3.0.2.2 Composite Concrete-Steel Deck

The bridge deck resists bending moment, axial forces, and shear forces. The design of the deck should achieve the following conditions:

- Bending Moment

$$g_2 = M_{fDeck} - M_{rDeck} \leq 0 \quad (3.7)$$

where M_{fDeck} , is factored bending moment in the deck and M_{rDeck} , is factored moment resistance of the composite section.

- Axial Tensile Forces

$$g_3 = T_{fDeck} - T_{rDeck} \leq 0 \quad (3.8)$$

where T_{fDeck} , is the factored tensile force in the deck and T_{rDeck} , is the factored tensile resistance of the deck.

- Axial Compression Force

$$g_4 = C_{fDeck} - C_{rDeck} \leq 0 \quad (3.9)$$

where C_{fDeck} , is the factored compressive force in the deck and C_{rDeck} , is the factored compressive resistance of the deck.

- Combined Axial and Bending Moment

The interaction diagram of the concrete steel deck cross-section is depicted in Fig. 3.4. The effect of both the axial load and bending moment on the deck girders are verified using the interaction diagram as given in Eq. (3.10).

$$g_5 = F_{(M_f, N_f)Deck} - F_{(M_r, N_r)Deck} \leq 0 \quad (3.10)$$

$$F_{(M_f, N_f)Deck} = \sqrt{M_{fDeck}^2 + C_{fDeck}^2} \quad (3.11)$$

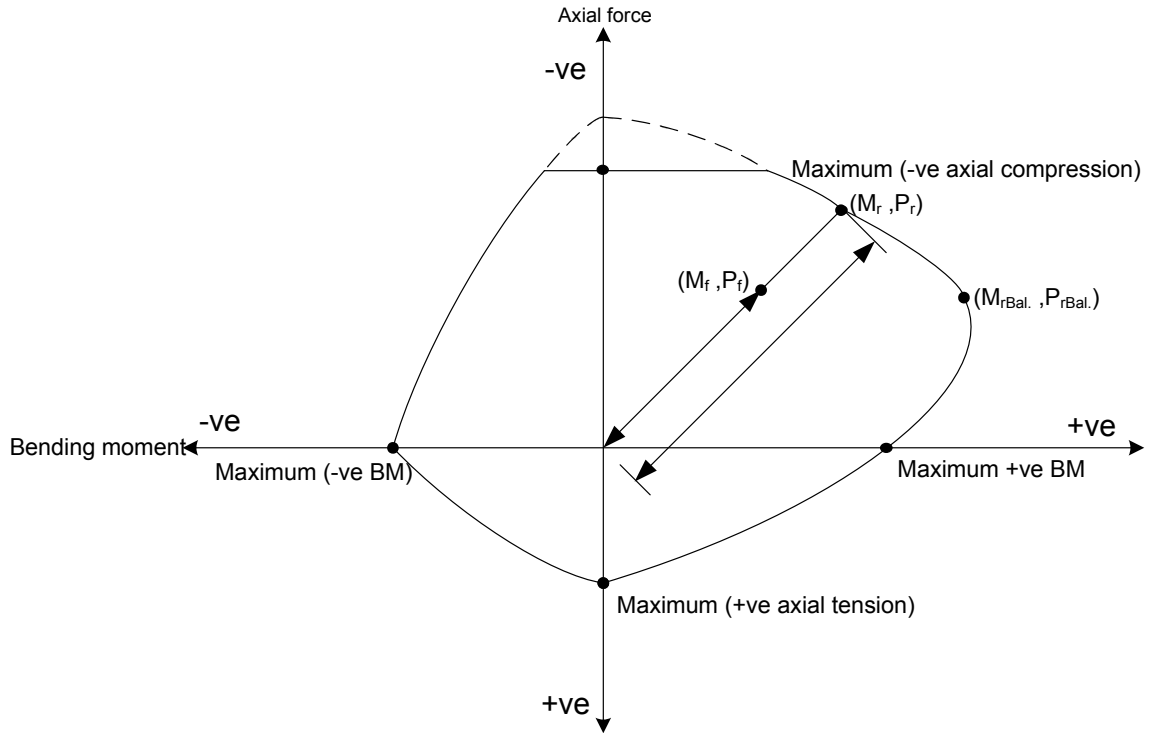


Figure 3.4: Interaction diagram of deck.

$$F_{(M_r, N_r)Deck} = \sqrt{M_{rDeck}^2 + C_{rDeck}^2} \quad (3.12)$$

where M_{fDeck} , is factored bending moment in the deck, C_{fDeck} is factored compressive force in the deck, M_{rDeck} is the factored moment resistance of the composite section, and C_{rDeck} , is the factored compressive resistance of the deck.

- Shear Force

$$g_6 = V_{fDeck} - V_{rDeck} \leq 0 \quad (3.13)$$

where V_{fDeck} is the factored shear force and V_{rDeck} , is factored shear resistance of the web steel main girder.

- Combined Shear and Moment

$$g_7 = 0.727 \frac{M_{fDeck}}{M_{rDeck}} + 0.455 \frac{V_{fDeck}}{V_{rDeck}} - 1 \leq 0 \quad (3.14)$$

where M_{fDeck} is factored bending moment in the deck, M_{rDeck} is the factored moment resistance of the composite section, V_{fDeck} is the factored shear force, and V_{rDeck} is the factored shear resistance of the web steel main girder.

- Deflection

The vertical deflections of the bridge deck under dead load are controlled by post-tension forces in the stay cables. The deflection criterion for long span bridges is not specified in CAN/CSA-S6-06 (2006). The following constraint given in the AASHTO.LRFD (2007) provides the maximum deflection criterion of the bridge deck under live load (Long et al., 1999)

$$g_8 = \frac{800\delta_{max}}{L} - 1 \leq 0 \quad (3.15)$$

where δ_{max} is the maximum deflection limit of the bridge deck due to live load and $\frac{L}{800}$ is the allowable deflection limit prescribed by AASHTO.LRFD (2007), and L is the total length of the bridge.

3.0.2.3 Pylon

The design of the pylon should achieve the following conditions:

- Buckling

The buckling capacities of the pylons are computed in both directions (longitudinal and transverse) of the bridge. The axial force in each pylon is computed and is then compared to the buckling capacities using the following equation:

$$g_9 = F_{fPylon} - F_{rPylon} \leq 0 \quad (3.16)$$

where F_{fPylon} is factored axial force in the pylon and F_{rPylon} is critical buckling capacity of the pylon.

- Axial Compression and Bending

The combined effect of the axial force and bending moment on the pylon are checked using the interaction diagram for the pylons cross-sections as follows in

$$g_{10} = F_{(M_f, N_f)Pylon} - F_{(M_r, N_r)Pylon} \leq 0 \quad (3.17)$$

$$F_{(M_f, N_f)Pylon} = \sqrt{M_{fPylon}^2 + P_{fPylon}^2} \quad (3.18)$$

$$F_{(M_r, N_r)Pylon} = \sqrt{M_{rPylon}^2 + P_{rPylon}^2} \quad (3.19)$$

where P_{fPylon} is the factored compressive force in the pylon, M_{fPylon} is the factored bending moment in the pylon, P_{rPylon} is the factored compressive resistance of the pylon, and M_{rPylon} is the factored moment resistance of the pylon.

3.1 Optimal Design Scheme

In this section, the scheme for optimal design is proposed based on an objective function and the finite element model.

3.1.1 Objective Function

The objective function which is denoted by (F) is the total cost of the cable-stayed bridge, including the cost of the stay cables, the structural concrete, and the structural steel. The objective function should be minimized and it can be defined as

$$F(x) = \gamma_{\text{cables}} \cdot V_{\text{cables}}(x) \cdot C_{\text{cables}} + V_c(x) \cdot C_{\text{concrete}} + \gamma_s \cdot V_{\text{steel}}(x) \cdot C_{\text{steel}} \quad (3.20)$$

where x is the design variables defined in (3.1). γ_{cables} and γ_s are the unit weight of stay cables and structural steel, respectively. V_{cables}, V_c , and V_{steel} , are the volume of cables, concrete, and structural steel, respectively. $C_{\text{cables}}, C_{\text{concrete}}$, and C_{steel} are the unit prices of stay cables, concrete, and steel, respectively (Hassan et al., 2012).

The unit prices of the bridge components used in this thesis include both the material cost and the construction cost. The prices are obtained from one of the major consulting firms (Hassan et al., 2012). Also, the unit prices of stay cables and structural steel depend on the weight, while that of concrete depends on the volume. These values can change from location to another and obviously they can vary with time. In Table 3.3, these values are presented.

3.1.2 Finite Element Model

The finite element models for three main arrangement of cable-stayed bridges are the same as the ones given in Chapter 2 and are plotted in Figs. 2.3a, 2.3, and 2.3c for semi-fan, fan, and harp arrangements, respectively. As one can see, the three main components, i.e., pylon, girder, and the stay cables are modeled using 3D line elements. A three-dimensional frame element is used to model the deck and the pylon, while a three-dimensional cable element is used to simulate the cables. Also, the deck is modeled using a single spine passing through its shear center. Moreover, the translational and rotational stiffness of the deck are calculated and are assigned to the frame elements of the spine. To achieve the proper offset of the cables from the centerline of the deck, the cable anchorages and the deck spine are connected by massless, horizontal rigid links (Wilson and Gravelle, 1991). These models will be incorporated in the next sections for optimal cost design of the three cable stayed arrangements.

3.1.3 Real Coded Genetic Algorithm

As explained before, the optimization technique and the cost optimization problem for cable-stayed bridges contains several local minima. Therefore, Genetic Algorithms (GAs) are employed in this study to find the global optimum solution for both arrangements of cable-stayed bridges. Note that genetic algorithms (GAs) based on the theory of biological evolution and adaptation have proved to be powerful, efficient, capable of handling large number of variables, and robust in finding global optimal solutions (Gen and Cheng, 2000). The real coded genetic algorithm (RCGA) is a variant of genetic algorithms that are suitable for the optimization of multiple-optima objective functions defined over continuous variables (Davis, 1991). The algorithm operates on the design variables, instead of encoding them into binary strings, as in the traditional genetic algorithms.

Genetic Operators

The mutation operators employed in Algorithm 3.1 allow the RCGA to avoid local minima. These operators search for solutions in remote areas of the objective function landscape (Hassan et al., 2012). The operators used in this study are the boundary mutation, non-uniform mutation, and uniform mutation. The boundary mutation searches the boundaries of the independent variables for optima lying there. Non-uniform mutation is a random search that decreases its random movements with the progress of the search. The Uniform mutation is a random search element. The crossover operators produce new solutions from parent solutions having good objective function values. In this study, it is used to produce new bridges from pairs of low cost bridge. The crossover operators used are the arithmetic, uniform and heuristic crossovers. The first produces new solutions in the functional landscape of the parent solutions. Details of such operators are given by Michalewics and Fogel (2004) and recently employed in Hassan et al. (2012). The above operators are applied on each

population with the following values: 1) Population size = 100 solution instances 2) 4 instances undergo boundary mutation. 3) 4 instances undergo non-uniform mutation. 4) 4 instances undergo uniform mutation. 5) 2 instances undergo arithmetic crossover. 6) 2 instances undergo uniform crossover. 7) 2 instances undergo heuristic crossover.

3.1.4 Post-tensioning Cable Forces

In the previous chapter, a numerical method is employed to obtain the post-tensioning cable forces for specific number of cables N , mid-span length M , and height of the pylon H . These forces are implemented in the analysis/design scheme employed in this chapter. However, in the design optimization process, the variables N , M , and H , can be assigned some random values that do not match the values considered in Chapter 2. To overcome this issue, three-dimensional linear interpolation (N , M , and H) is conducted between the data points for the forces of post-tensioning cable forces evaluated in Chapter 2.

3.1.5 Load Considerations

Dead load, wind load, and live load are considered in this thesis based on Canadian Highway Bridge Design Code (CAN/CSA-S6-06, 2006).

3.1.5.1 Dead Load

According to clause 3.6 of the CAN/CSA-S6-06 (2006), the dead load of the bridge contains the structural weight of the bridge, a thickness of 0.09 m layer of asphalt, and two concrete traffic barriers having an average thickness and height of 0.325 m and 0.85 m, respectively.

3.1.5.2 Live Load

To compute the live load acting on the bridge deck using clause 3.8.3.2 of the CAN/CSA-S6-06 (2006) the following two cases are considered:

- CL-W truck.
- CL-W truck with each axle reduced to 80% and superimposed with a uniformly distributed load ($q_L = 9kN/m$) lane.

In short and medium span cable-stayed bridges, the main effect always results due to a single axle, group of axles, or single truck. For long span cable-stayed bridges, the critical force effect and largest deflection are due to the distributed lane loads. Hence, the live load acting on the bridge deck in this study is given as:

$$Liveload = m_F n_{Lane} q_L \quad (3.21)$$

where m_F is the modification factor used when more than one design lane is loaded according to clause 3.8.4.2, and Table 3.8.4.2, of CAN/CSA-S6-06 (2006), n_{Lane} , is the number of the lanes, and $q_L = 9kN/m$ is the uniformly distributed load.

The nine live load configurations applied to determine the optimum cost design of three type of the cable-stayed bridge are shown in Fig. 3.5 (Walther et al., 1988).

The live load is calculated using Eq. (3.21). It has a magnitude equal to 16.2 kN/m and 25.2 kN/m for the case of two and four lanes, respectively CAN/CSA-S6-06 (2006)..

3.1.5.3 Wind Load

Cable-stayed bridges are considered sensitive to wind load. Therefore, wind tunnel tests are required to determine the lift (CN), torsional (CM), and drag (CD) shape coefficients of the deck. Based on clause 3.10.5 of (CAN/CSA-S6-06, 2006), the wind load is computed as follows:

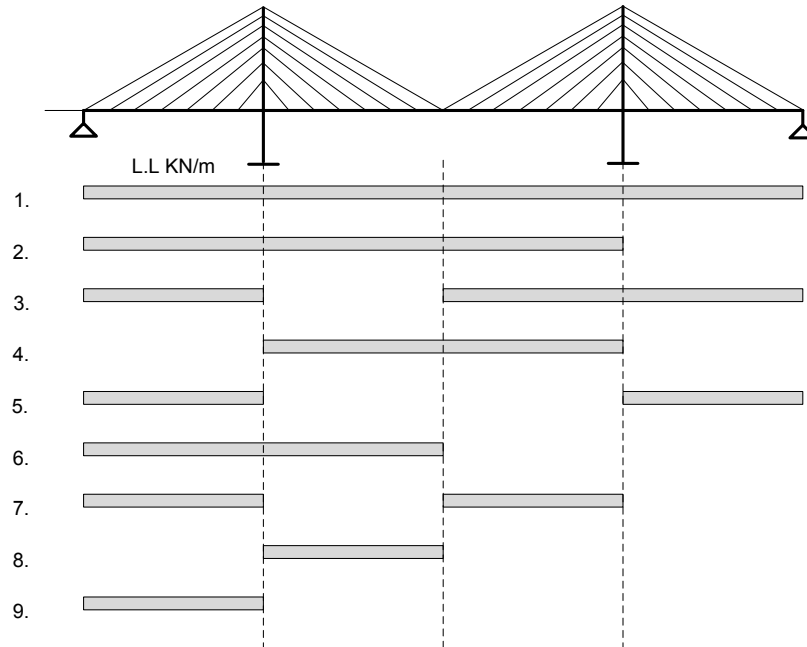


Figure 3.5: Live load cases used in the numerical model(Hassan et al., 2012).

$$q_{wT} = C_T q h \quad (3.22)$$

$$q_{wM} = C_M q h B \quad (3.23)$$

$$q_{wD} = C_D q h \quad (3.24)$$

where h is the wind exposure depth B is the width of the deck, C_N is the lift shape coefficients of the deck, C_M is the torsional shape coefficients of the deck, C_D is the drag shape coefficients of the deck, and q is the hourly mean reference wind pressure according to the clause 3.10.1.1 of (CAN/CSA-S6-06, 2006). Also, q_{wT} is wind load due to lift, q_{wM} is wind load due to torsional shape, and q_{wD} is wind load due to drag shape (Hassan, 2010). It is assumed that the bridge is located in Victoria, British Colombia, CANADA. The angle of attack of the wind on the deck is assumed to be zero and hence only the drag pressure, i.e., q_{wD} is included in this thesis.

For the mentioned location, $q_{wD} = 690 \text{ N/m}^2$, as specified in the (CAN/CSA-S6-06, 2006). Also, the drag coefficients of the deck C_D is assumed to be equal to 0.8 as recommended by Walther et al. (1988).

3.1.5.4 Load Factors and Combinations

According to Tables 3.5.1 (a) of the CAN/CSA-S6-06 (2006), the load factors and combinations are as follows:

$$1.1D + 1.7L \quad (3.25)$$

$$1.1D + 1.4L + 0.5W \quad (3.26)$$

$$1.1D + 1.65W \quad (3.27)$$

where D is the dead load, L is the live load., and W is the wind load.

3.1.6 The Cost Optimization Algorithm

The sequences for obtaining an optimum design cost is given in Algorithm 3.1 by Hasan et al. (2012). The algorithm combines the finite element model, three dimensional linear interpolation, design methodologies, and real coded genetic algorithm (RCGA) to obtain optimum design cost for cable-stayed bridges. In the current study, is treated for two different arrangements including fan and harp arrangements. First, it reads the lower bounds and upper bounds for the design variables. Then, it determines the post-tensioning cable forces for two arrangements. The three dimensional linear interpolation described in Section 3.1.4 is used to obtain the post-tensioning cable forces for the optimum design cost. Detailed explanation of Algorithm 3.1 is given below:

Algorithm 3.1 Modified Optimum Cost Design Algorithm Hassan et al. (2012)

Inputs: Population size 100, operators, LB and UB of the design variables

Outputs: The cable-stayed bridge with the smallest cost value

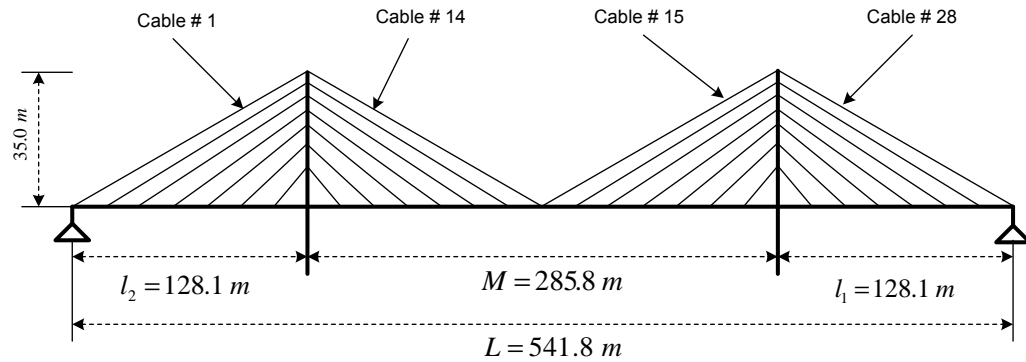
0. Initialize $G = 1$ as the number of generations
1. While $G \leq G_{max}$ do the following
 - 1.1 Develop the 3D FEM model for each cable-stayed bridge
 - 1.2. Calculate the post-tensioning cable forces using three dimensional linear interpolation
 - 1.3. Apply the post-tensioning cable forces with the other loads to the FEM.
 - 1.4 Calculate the objective function $F(x)$ (given in Eq. (3.20)) value
 - 1.5 Sort the population in an ascending order to the value of the objective function $F(x)$
 - 1.6. Set $G = G + 1$.
 - 1.7. Generate a new populations and design variables
2. else
3. Return the cost with the smallest value of $F(x)$

-
1. Generate an initial population of the design variables defined in Section 3.0.1, randomly selected by the (RCGA) algorithm between the lower and upper bounds of each design variable. The design variables define the geometric configuration, the number of stay cables, and cross-sectional dimensions of the bridge.
 2. Develop a 3-D finite element model (FEM) for each search case in the population for fan and harp arrangements of cable-stayed bridges given in Section 3.1.2.
 3. Calculate the post-tensioning cable forces in each stay cable using the post-tensioning three dimensional linear interpolation described in Section 3.1.4. Apply these forces to the 3-D FEM together with other types of loads, including dead, live, and wind loads, and analyze the structure to determine the internal forces and displacements of the bridge components.

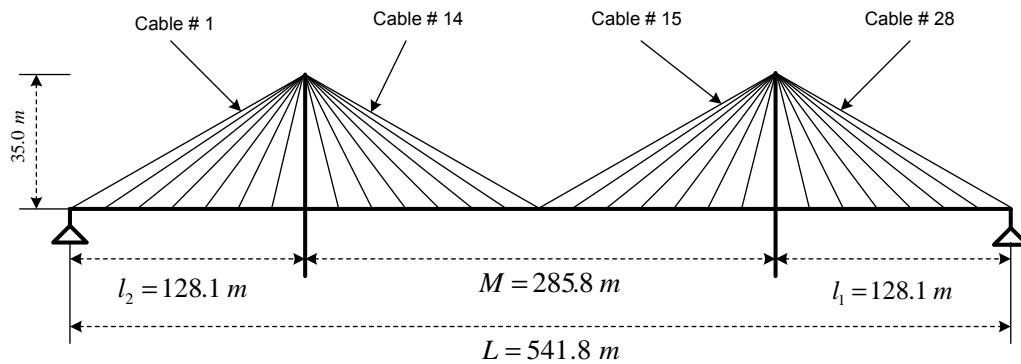
4. Check that internal forces and displacements in Step 3 satisfy the design constraints defined in Section 3.0.2. If any of these constraints are not satisfied, the result of this specific bridge is excluded.
5. Sort the initial population in ascending order according to the value of the objective function such that the first ranked candidate cable-stayed bridge has the minimum value of the feasible cost design.
6. Use genetic algorithm and generate a new population by applying the crossover and mutation operators on the high ranked cost functions evaluated at Step 5 to produce a new generation as required. These operators direct the search towards the global optimum solution.
7. Replace the previous population with the newer one containing the new candidate cable-stayed bridges, in addition to the best candidate cable-stayed bridge found in previous steps.
8. Repeat Steps 2 to 7 for a certain number of generations, taken as 100 iterations until a global optimum solution is obtained.
9. Deliver the candidate cable-stayed bridge with smallest values of the objective function F obtained at Step 8 as the final solution.

3.1.7 Description of the Bridge for Semi-fan, Fan and Harp Arrangement

The bridge that is considered in this thesis is the semi-fan Quincy Bayview Bridge as described in Chapter 2. The configuration of this bridge is modified to form two other arrangements, i.e., fan and harp styles. It is assumed that the deck has two traffic lanes, i.e., $n_{\text{Lanes}} = 2$. The total width of the precast slab is $B = 14.20$ m as shown in Fig. 3.2a. Two steel main girders are connected to the deck as shown in Fig. 3.2b.



(a) Harp arrangement



(b) Fan Arrangement

Figure 3.6: Alternative arrangements of Quincy Bayview Bridge

In the semi-fan arrangement, the distance between the stay cables anchorages along the pylon is 2.0 m. While, in the fan type all the stay cables are connected in top of the pylon. In the harp type, the distances between the cables on the pylon depends on the number of the stay cables. Therefore, the distance between stay cables on the pylon for harp arrangement is obtained by dividing the upper strut height to the number of cables.

Table 3.3: Material Properties of the bridge

Material	Parameter	Definition	Properties
Steel	E_s	Modulus of elasticity	200 GPa
	γ_s	Unit weight	77 kN/m^3
	ν_s	Poisson's ratio	0.3
	F_y	Yield strength	350 MPa
	C_{steel}	Unit price	12,000 \$/ton
Concrete	E_c	Modulus of elasticity	24.87 GPa
	γ_c	Unit weight	24 kN/m^3
	ν_c	Poisson's ratio	0.2
	$f_{c'}$	Compressive strength	30 MPa
	C_{concrete}	Unit price	4,218 \$/m ³
Cables	E_{sc}	Modulus of elasticity	205 GPa
	γ_{cable}	Unit weight	82.40 kN/m^3
	T_{cable}	Ultimate tensile strength	1.6 GPa
	C_{cable}	Unit price	60,000 \$/ton
Reinforcement steel	f_y	Yield strength	400 MPa
Asphalt	γ_{asphalt}	Unit weight	23.5 kN/m^3

The total length of the bridge is $L = 542$ m for both arrangements as shown in Fig. 3.6. The two pylons are H-shaped similar to the original bridge, with a width of $d = 13.28$ m. Other geometric parameters, design parameters, are illustrated as shown in Fig. 3.6a and Fig. 3.6b, for the harp and fan arrangements, respectively. Based on CAN/CSA-S6-06 (2006), a layer of asphalt having a thickness of 0.09 m, two concrete traffic barriers with the average thickness of 0.325 m and 0.85 m are added as the dead loads and structural self-weight of the bridge. The floor cross beams with a load per unit area of 0.75 kN/m^2 is added too. It should be noted that

the self-weight of the bridge varies for different optimization cases, since it depends on the cross sectional design variables of the deck and the pylon. The magnitude of the live load is based on the information given in Eq. (3.21) and is equal 16.2 kN/m .

In the simulations, the top part of the pylons for fan and harp arrangements is removed. The properties and unit prices of the materials used in this work are tabulated in Table 3.3.

3.2 Results

In this section, the results for the optimum cost design of the three arrangements of cable-stayed bridges including semi-fan, fan, and harp arrangements are presented. The effect of different geometric configurations on bridge components cost (pylon, deck, cables, and total cost) as well as the number of stay cables are investigated for these arrangements.

3.2.1 Reference Costs of Quincy Bayview Bridge

In the study conducted by Hassan (2010) an optimization for the cross section of the Quincy Bayview Bridge was conducted for a semi-fan arrangement while the number of stay cables (N), main span length (M), and the height of the pylon (H), are kept constant with the values used in the real bridge. The cost obtained from this optimization is considered in the current study as the reference cost. The values of the design variables and the cost of the reference bridge are presented in Table 3.4 showing a total value of \$ 28,512,194 (Hassan, 2010).

Table 3.4: Reference Cost of Quincy Bayview Bridge(Hassan, 2010)

Design variables	Definition	Semi-fan
N	Number of stay cables in each single plan	7
γ_1	mid - span length / bridge length	0.52
γ_2	upper strut height / bridge length	0.065
D_{max}	Maximum diameter of the cables	0.08 m
D_{min}	Minimum diameter of the cables	0.05 m
t_s	Thickness of concrete deck slab	0.15 m
H_G	Height of the two steel main girders	2.90 m
B_{FT}	Width of top flange	0.551 m
B_{FB}	Width of bottom flange	0.638 m
t_{FT}	Thickness of upper flange	0.035 m
t_{FB}	Thickness of lower flange	0.037 m
t_w	Thickness of web	0.018 m
H_P	Pylon depth	3.5 m
B_P	Pylon width	1.5 m
t_P	Pylon thickness	0.50 m
cost	Pylons cost	\$ 3,306,912
cost	Deck cost	\$ 13,999,430
cost	Cables cost	\$ 11,205,851
cost	Total cost	\$ 28,512,194

3.2.2 Comparison of the Optimal Cost of Different Arrangements

In this section, the optimal design of the bridge is determined by allowing all the design variables (including N , M , and H) to vary between the upper and lower bound described in Table 3.2. The post-tensioning cable forces are obtained using a three-dimensional linear interpolation between the data point developed in Chapter 2 as mentioned before. The results of the minimum cost design of the bridge and optimum values of the design variables for harp, fan, and semi-fan (done by Hassan (2010)) arrangements are presented in Table 3.5. The three main arrangements, i.e., fan, semi-fan, and harp are compared in terms of optimum design variables as well as the optimum design costs to the reference bridge (Quincy Bayview Bridge described in Section 3.2.1). As one can see, the semi-fan arrangement has the lowest cost in comparison to the other arrangements. The total cost of the reference bridge is \$28,512,194 while the costs of the semi-fan, fan, and harp arrangements are \$24,215,214.00 (obtained by Hassan (2010)), \$29,412,915.00, and \$38,628,224.00, respectively. The total cost of semi-fan arrangement is 15% less than the reference bridge and has the lowest cost. The fan arrangements has 3% more cost in comparison to the reference bridge and the harp arrangement is the most expensive arrangement and its total cost is 26% more than the reference bridge. It should be noted that the optimal numbers of stay cables are 8, 8, and 8, for semi-fan, fan, and harp arrangements, respectively. It can be noticed from the results that, in spite of increasing the number of stay cables from 7 to 8, a reduction in the stay cables cost of 23.8% is achieved for the optimized semi-fan arrangement done by Hassan et al. (2012) in comparison to the reference bridge. For fan arrangement, 8 cables provide the optimal design and its cable cost is about 6.4% and 28% more than the reference bridge, and the optimized semi-fan arrangement, respectively. The cables cost for the harp arrangement is 37% and 52% more than the reference bridge, and the optimized

semi-fan arrangement, respectively.

3.2.3 Effect of Geometric Configuration on the Bridge Cost

In this subsection, a parametric study is conducted to assess how the optimum design of the bridge varies with various geometric parameters. Following parameters are considered in this study:

- The ratio of mid-span length and total length of the bridge denoted by $\gamma_1 = \frac{M}{L}$.
- The ratio of upper strut and total length of the bridge denoted by $\gamma_2 = \frac{h_B}{L}$ as shown in Table 3.6.

In the following, the results for $\gamma_1 = \frac{M}{L} \in \{0.48, 0.50, 0.52, 0.54\}$, and $\gamma_2 = \frac{h_B}{L} \in \{0.037, 0.055, 0.074, 0.11\}$ are obtained for fan and harp arrangements. The number of stay cables N , is maintained as 7 in this subsection. The value for these design variables are shown in Table 3.6.

3.2.3.1 Effect of Geometric Configuration on the Pylon Cost

The effect of variation of the pylon height (which is done by varying γ_2) on the pylon cost is illustrated in Fig. 3.7. As one can see, for different values of $\gamma_1 = \frac{M}{L}$, as the pylon height increases the pylon cost increases as well due to the usage of more materials. One should note that this increase in the cost is independent of γ_1 (ratio of mid-span length and total length of the bridge) for the three arrangements. For each main span value, a set of post-tensioning forces is applied leading to minimum deflection and minimum bending moment along the pylon. Hence, the structural behaviour of the pylon, and consequently its cost, remains unchanged with the variation of the main span.

Table 3.5: Comparison of the optimal solutions for three types of the cable-stayed bridges

Design vars.	Definition	Values for Ref. bridge (Hassan, 2010)	Values for Semi-fan (Hassan, 2010)	Values for Fan	Values for Harp
N	Number of cables in each plan	7	8	8	8
γ_1	mid - span length / bridge length	0.506	0.481	0.48	0.53
γ_2	upper strut height / bridge length	0.065	0.109	0.10	0.11
D_{max}	Max. diameter of the cables	0.08 m	0.07 m	0.09 m	0.15 m
D_{min}	Min. diameter of the cables	0.05 m	0.03 m	0.05 m	0.05 m
t_s	Thickness of concrete deck	0.15 m	0.15 m	0.16 m	0.21 m
H_G	Height of the two steel main girders	2.90 m	2.507 m	2.45 m	3.10 m
B_{FT}	Width of top flange	0.551 m	0.417 m	0.501 m	0.601 m
B_{FB}	Width of bottom flange	0.638 m	0.510 m	0.602 m	0.652 m
t_{FT}	Thickness of upper flange	0.035 m	0.021 m	0.028 m	0.039 m
t_{FB}	Thickness of lower flange	0.037 m	0.029 m	0.035 m	0.041 m
t_w	Thickness of web	0.018 m	0.016 m	0.017m	0.02 m
H_P	Pylon depth	3.5 m	4.0 m	3.5 m	4.0 m
B_P	Pylon width	1.5 m	2.0 m	2.0 m	1.5 m
t_P	Pylon thickness	0.50 m	0.5 m	0.5 m	0.5 m
cost	Pylons cost	\$ 3,306,912	\$ 4,946,085	\$ 4,797,760	\$ 4,798,121
cost	Deck cost	\$ 13,999,430	\$ 10,740,590	\$12,640,362	\$15,824,377
cost	Cables cost	\$ 11,205,851	\$ 8,528,538	\$11,974,794	\$18, 005, 726
cost	Total cost	\$ 28,512,194	\$ 24,215,214	\$29,412915	\$ 38,628,224

Table 3.6: Parameters used to study effect of geometric configuration on the bridge cost.

Design variables	Definition	Values
N	Number of stay cables in each single plan	7
γ_1	mid - span length / bridge length	0.48, 0.50, 0.52, 0.54
γ_2	upper strut height / bridge length	0.037, 0.055, 0.074, 0.11

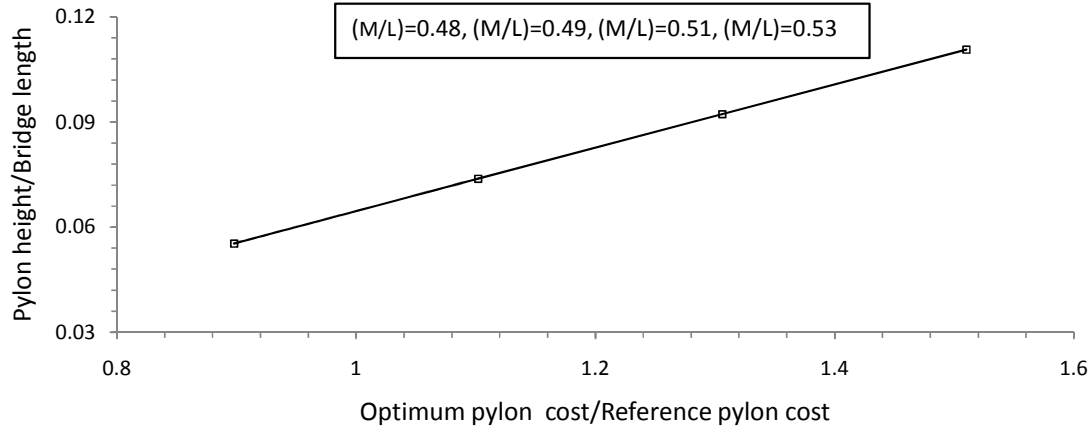


Figure 3.7: Variation of pylon cost with height of the pylon and main span length in fan and harp arrangements. Note that $N = 7$ and $\gamma_1 = \frac{M}{L} \in \{0.48, 0.50, 0.52, 0.54\}$.

3.2.3.2 Effect of Geometric Configuration on the Deck Cost

In this subsection, the effect of variation of the deck cost with the height of the pylon (γ_2) and the mid-span length (γ_1) for the fan and harp arrangements is investigated. The results are illustrated in Fig. 3.9a. Note that the results for the semi-fan arrangement are already given by Hassan (2010). As shown in this figure, for the various ratios of γ_1 , as the pylon height γ_2 increases, the deck cost reduces significantly. This is due to the fact that the increase in the pylon height reduces the moments and horizontal forces on the deck and consequently reduces the thickness of the deck, which leads to a relatively small deck cross-section. The reduction in γ_1 results in having minimum deck cost as well. In Fig. 3.9b, the effect of the variation of the pylon height and main span length on the deck cost for harp arrangement is investigated. As one can see, the optimum deck cost reduces as the pylon height increases simi-

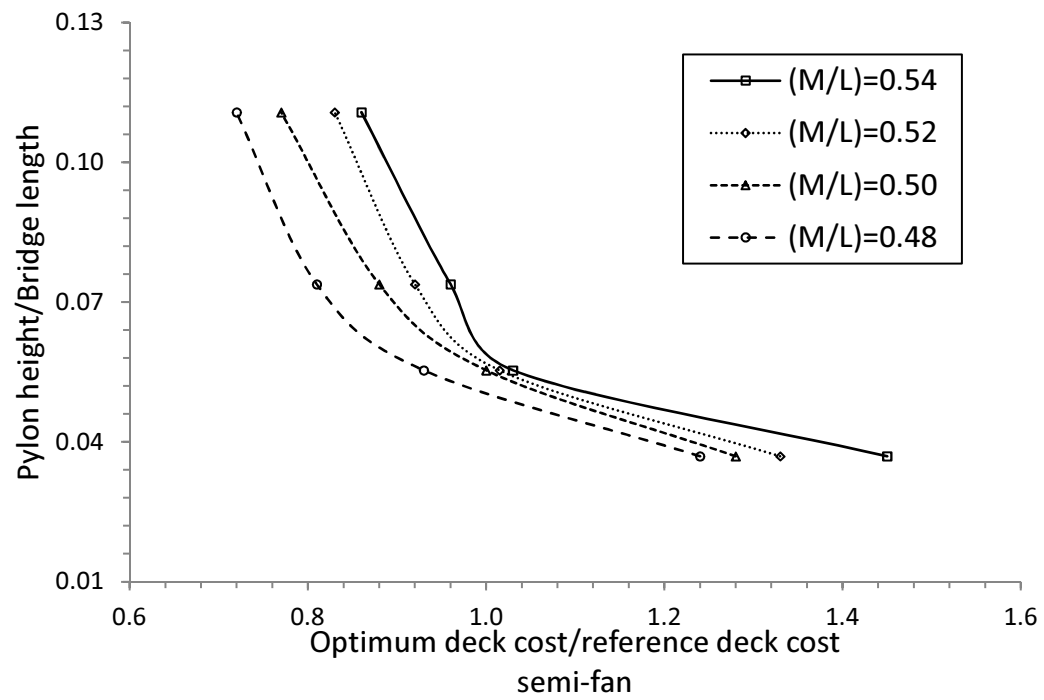
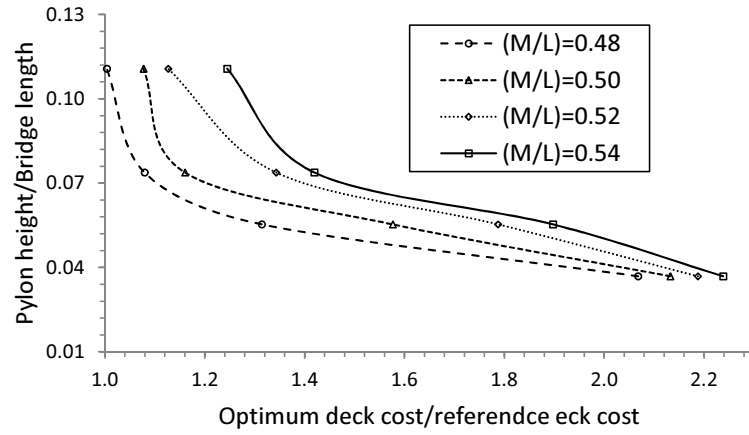
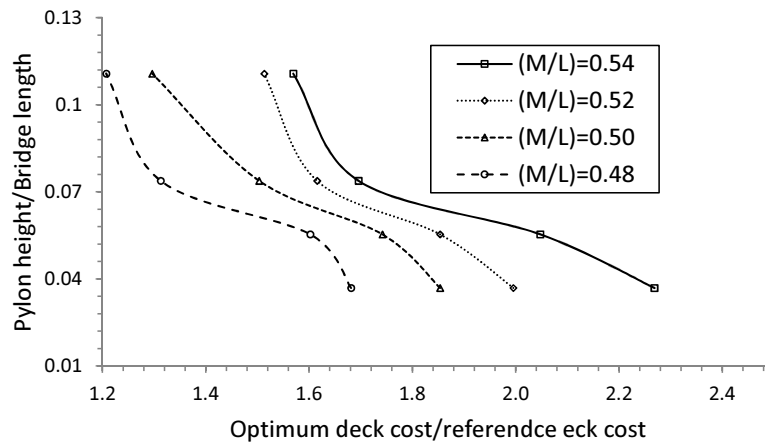


Figure 3.8: Variation of deck cost with height of the pylon and main span length for the semi-fan arrangement.



(a) Fan arrangement



(b) Harp arrangement

Figure 3.9: Variation of deck cost with height of the pylon and main span length for the fan and harp arrangements. Note that $N = 7$, $\gamma_1 = \frac{M}{L} \in \{0.48, 0.50, 0.52, 0.54\}$, and $\gamma_2 = \frac{h_B}{L} \in \{0.037, 0.055, 0.074, 0.11\}$.

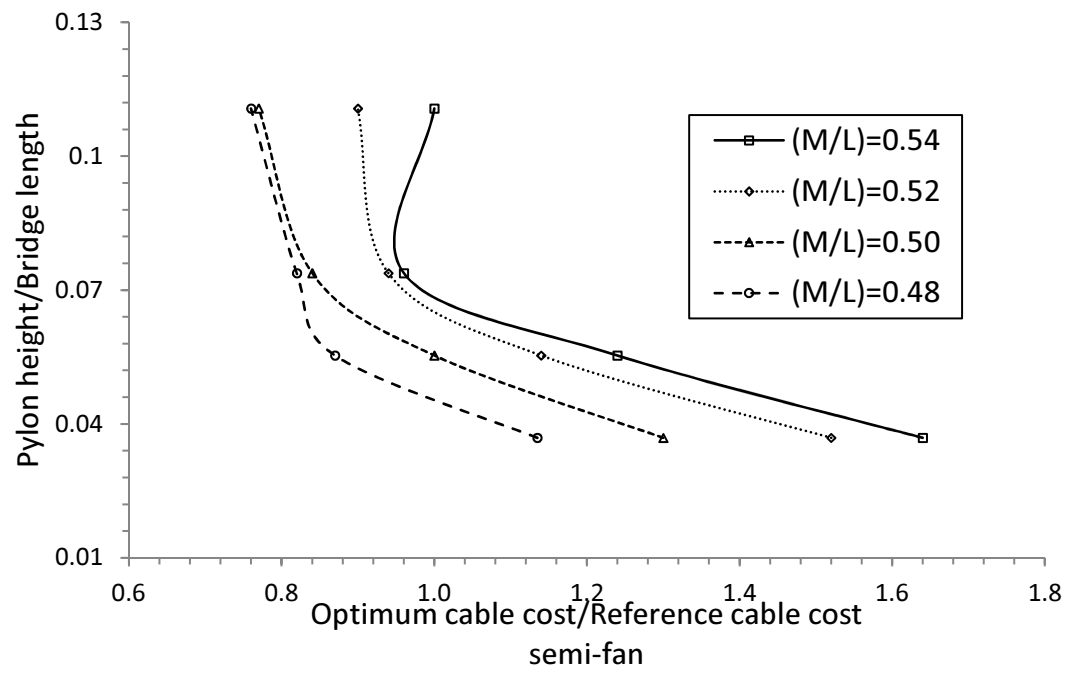
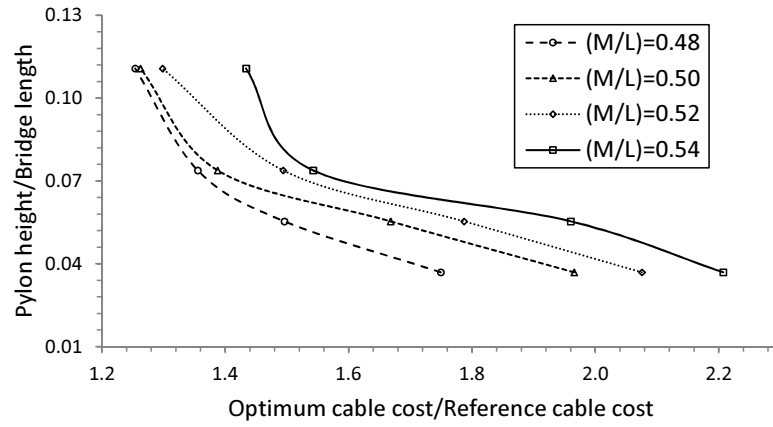
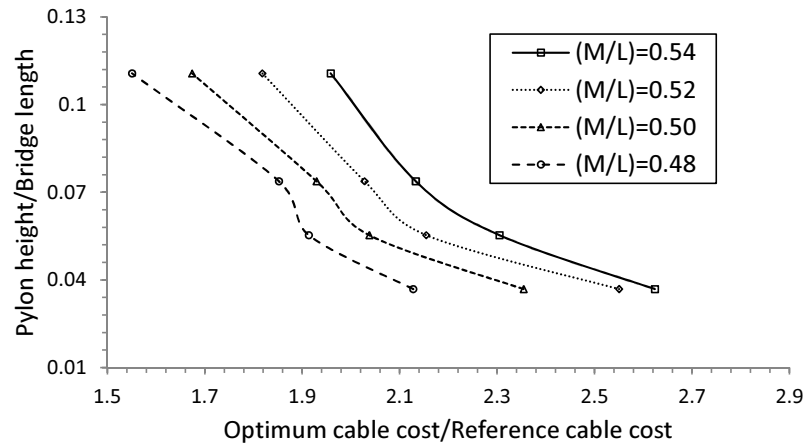


Figure 3.10: Variation of stay cables cost with height of the pylon and main span length for semi-fan arrangement.



(a) Fan arrangement



(b) Harp arrangement

Figure 3.11: Variation of stay cables cost with height of the pylon and main span length for the harp and fan arrangements. Note that $N = 7$, $\gamma_1 = \frac{M}{L} \in \{0.48, 0.50, 0.52, 0.54\}$, and $\gamma_2 = \frac{h_B}{L} \in \{0.037, 0.055, 0.074, 0.11\}$.

lar to the fan arrangement. However, the cost of the deck is not reduced less than 1.2 times of the reference bridge due to the high post-tensioning cable forces in the harp arrangement. As an example, for $\gamma_1 = 0.48$ increasing the pylon height ratio γ_2 from 0.074 to 0.11 results in 7.7% reduction in the cost of the deck in the harp arrangement. For larger value of γ_2 , ($\gamma_2 = \frac{h_B}{L} = 0.11$) and for $\gamma_1 = \frac{M}{L} = 0.54$ the ratios between the optimum deck cost and the reference cost are 0.88, 1.24, and 1.56 for semi-fan, fan, and harp arrangements, respectively. Also, for the minimum value of γ_2 , ($\gamma_2 = \frac{h_B}{L} = 0.037$) with $\gamma_1 = 0.54$, the ratios between optimum deck costs and the reference deck costs are 1.44, 2.24, and 2.27, for semi-fan, fan, and harp arrangements, respectively.

The results indicate that increasing the pylon height reduces the optimum deck cost of three arrangements. Moreover, the optimum deck cost reduces as the mid-span length γ_1 reduces. It can be concluded that, the variation of geometric configurations has more impact on the optimum deck cost for the harp arrangement. Also, as expected, semi-fan arrangement achieves the lowest cost in comparison to the other two arrangements.

3.2.3.3 Effect of Geometric Configuration on the Cables Cost

In Fig. 3.11a, the variation of stay cables cost with the height of the pylon and mid-span length for the fan arrangement is illustrated. As has been mentioned in chapter 2, the increase in pylon height results in reduction in the post-tensioning cable forces (Troitsky, 1988). This directly reduces the diameters of stay cables and the compressive forces acting on the deck and the pylons. Therefore, the diameter of the cables will be smaller. However, this enlarges the pylon height, and the stay cables lengths. Also, it can be noted from the figure that the reduction of the γ_1 ratio reduces the stay cables cost. However, this reduction is not linear. For instance, the reduction of the ratio of mid-span length and total length of the bridge from 0.54 to

0.52 (γ_1) results in a significant reduction of the stay cables costs. However, more reduction in γ_1 from 0.52 to 0.48 does not reduce the cost of stay cables remarkably as illustrated in Fig. 3.11a. Therefore, to achieve an optimum design cost for the fan type stay cables one needs to compromise on the selection of γ_1 . In Fig. 3.11b, the effect of the variation of pylon height and main span length on the cost of stay cables for harp arrangement is illustrated. Similar to the fan arrangement, as the pylon height increases, the optimum cost of cable forces reduces. One can achieve more reduction in the cost of stay cable by reducing the values of γ_1 as shown in this figure. In comparison to the fan arrangement, the cost of cable forces are higher for harp arrangement. As seen, in the worst case having $\gamma_1 = 0.54$ and $\gamma_2 = 0.037$, the cost of the harp arrangement is 2.6 times the reference bridge, which is 15% more than the fan arrangement having $\gamma_1 = 0.54$ and $\gamma_2 = 0.037$.

For the larger values of γ_2 , ($\gamma_2 = \frac{h_B}{L} = 0.11$) with $\gamma_1 = \frac{M}{L} = 0.54$, the ratios of the optimum cable costs and the reference cable costs are 1.0, 1.44, and 1.94 for semi-fan, fan, and harp arrangements, respectively. Also, for the minimum value of γ_2 , ($\gamma_2 = \frac{h_B}{L} = 0.037$) with $\gamma_1 = 0.54$, the ratios of the optimum cable costs and the reference cable costs are 1.64, 2.2, and 2.62, for semi-fan, fan, and harp arrangements, respectively.

3.2.3.4 Effect of Geometric Configuration on the Bridge Cost

In this subsection, the effect of the variation of the pylon height on the optimum bridge cost is investigated. In Fig. 3.13a, variation of the pylon height ($\gamma_2 = \frac{h_B}{L} \in \{0.037, 0.055, 0.074, 0.11\}$) and main span length ($\gamma_1 = \frac{M}{L} \in \{0.48, 0.50, 0.52, 0.54\}$) on the optimum bridge cost is illustrated for fan arrangement. As one can see, as the pylon height increases, the optimum cost of the bridge decreases significantly. Also, decreasing γ_1 results in a reduction in the optimum cost of the bridge. In Fig. 3.13b, the effect of variation of the pylon height γ_2 and the ratio of mid-span length

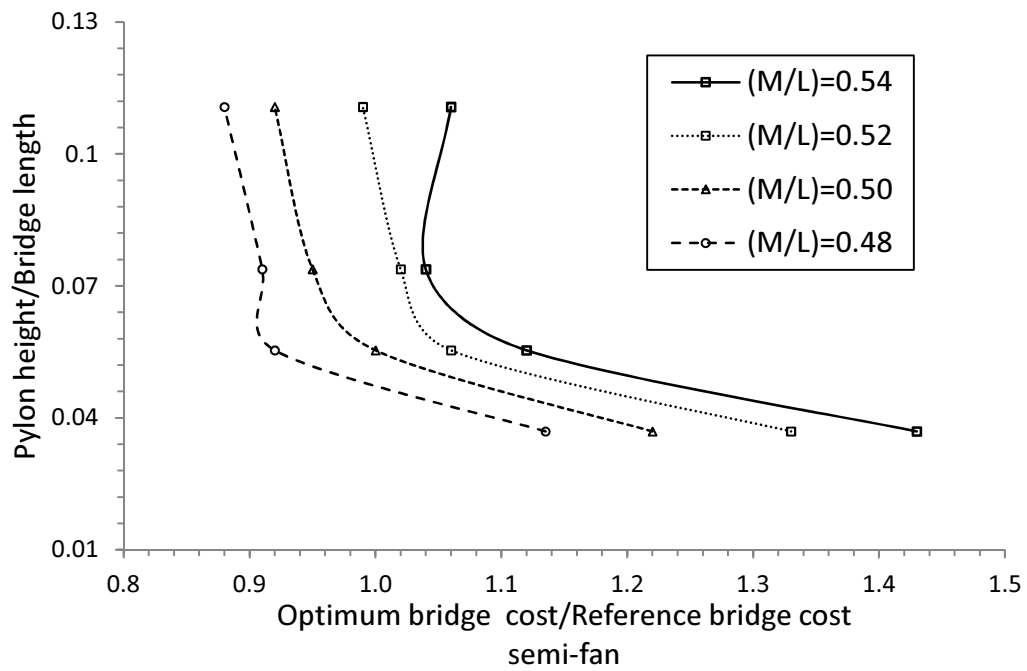
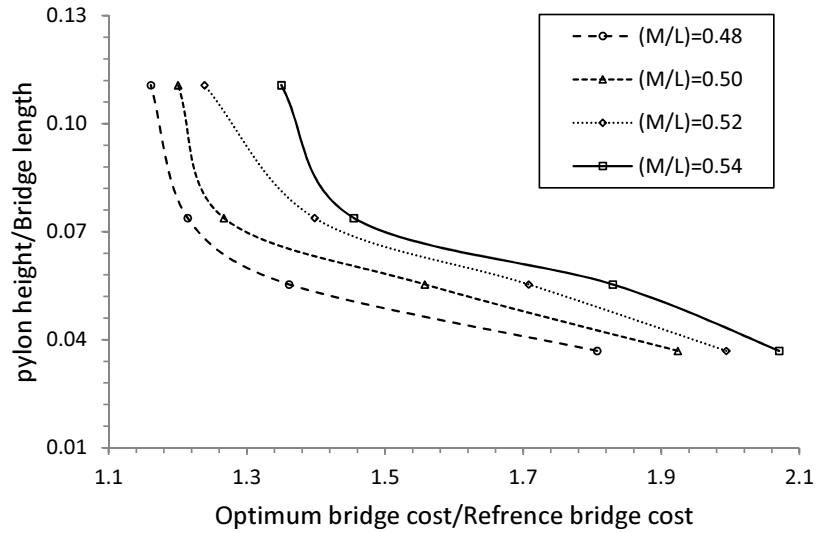
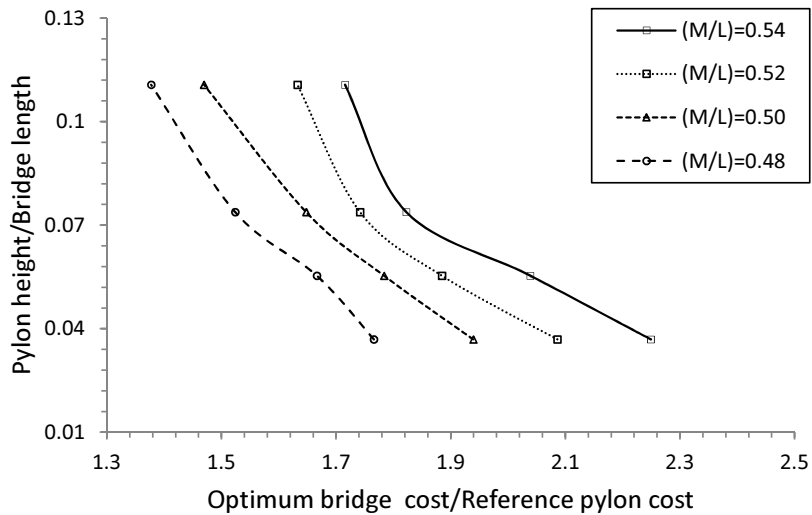


Figure 3.12: Variation of bridge cost with height of the pylon and main span length for semi-fan arrangement.



(a) Fan Arrangement



(b) Harp arrangement

Figure 3.13: Variation of bridge cost with height of the pylon and main span length for the fan and harp arrangements. Note that $N = 7$, $\gamma_1 = \frac{M}{L} \in \{0.48, 0.50, 0.52, 0.54\}$, and $\gamma_2 = \frac{h_B}{L} \in \{0.037, 0.055, 0.074, 0.11\}$.

to the total length, γ_1 on the total bridge cost is illustrated for the harp arrangement. Similar to the fan arrangement, as the pylon height increases the optimum cost of the harp arrangement decreases significantly. Also, increasing the ratio of mid-span length and total length of the bridge in the range of 0.48 to 0.54 increases the bridge cost as well. For the larger values of γ_2 , ($\gamma_2 = \frac{h_B}{L} = 0.11$) with $\gamma_1 = \frac{M}{L} = 0.54$, the ratios of optimum bridge cost and the reference bridge cost are 1.08, 1.35, and 1.74 for semi-fan, fan, and harp arrangements, respectively. Also, for the minimum value of γ_2 , ($\gamma_2 = \frac{h_B}{L} = 0.037$) with $\gamma_1 = 0.54$, the ratios of the optimum bridge costs and the reference bridge cost are 1.44, 2.09, and 2.26, for semi-fan, fan, and harp arrangements, respectively.

In comparison to the semi-fan arrangement presented in Fig. 3.13, the optimum bridge costs are higher for the harp and fan arrangements. However, depending to the applications, there are some case that it is possible to take advantages of fan and harp arrangements favorably comparable to the semi-fan arrangement. For example, in fan arrangement, by taking $\gamma_1 = 0.48$ and $\gamma_2 = 0.074$, the normalized optimum bridge cost is 1.16 which can be achieved with larger γ_1 ratios for semi-fan arrangement.

As illustrated in Fig. 3.13, the optimum cost of the bridge reduces and it is possible to achieve more reduction by reducing the pylon height. Therefore, to achieve optimum cost one should consider these two parameters and make a compromise. In comparison to the optimum cost of the bridge for fan arrangement, the harp arrangement has higher cost. Recall that the post-tensioning cable forces for harp arrangement are higher than fan arrangement.

3.2.4 Effect of Number of Cables on the Bridge Cost

The choice of the number of stay cables supporting the deck is considered as one of the most important factors in the design process for a cable-stayed bridge. As mentioned before, the increase in the number of stay cables decreases the length

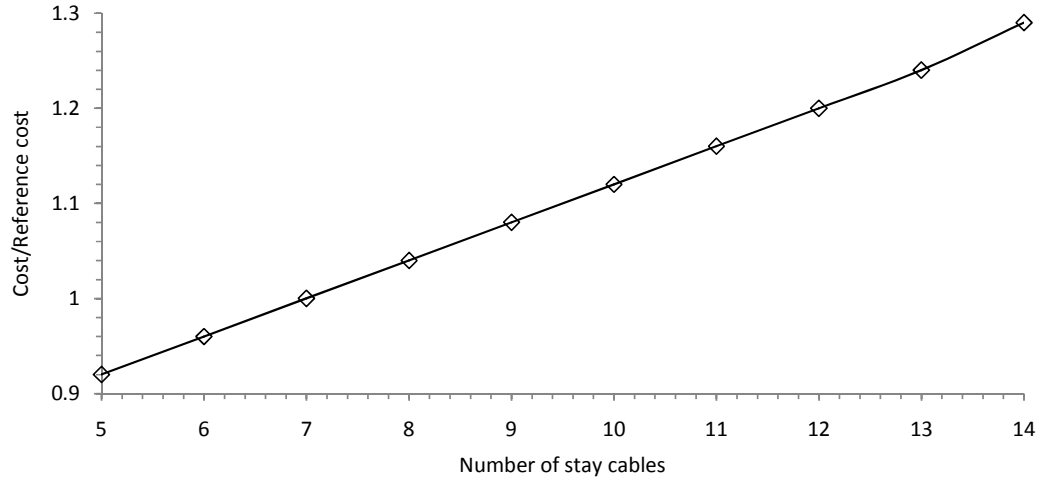


Figure 3.14: Variation of Pylon cost with number of stay cables in three types of cable-stayed bridges. Note that $N = \{5, 6, 7, 8, 9, 10, 11, 12, 13, 14\}$, $\gamma_1 = 0.52$, and $\gamma_2 = 0.083$.

between two consecutive stay cables, which reduces the bending moment along the longitudinal direction of the deck and the deck cross-section. Moreover, this increase reduces the post-tensioning cable forces, which reduces the stresses concentration at the anchorage points in the pylon and deck.

In this subsection, the effect of number of stay cables on the bridge cost for both the fan and harp arrangements are investigated. The number of stay cables are chosen from $N = \{5, 6, 7, 8, 9, 10, 11, 12, 13, 14\}$. The main span length (M), and height of the pylon (H) are equal to the Quincy Bayview Bridge. In Figs. 3.14, 3.15, 3.16, and 3.17, the effects of increasing the number of stay cables on the cost of pylon, deck, and stay cables are illustrated. In the following, the effect of number of cables are presented for different bridge component costs.

3.2.4.1 Effect of Number of Cables on the Pylon Cost

In Fig. 3.14, the effect of variation of the number of cables N , on the pylon cost is illustrated. The optimization analyses are repeated for various values of $N = \{5, 6, 7, 8, 9, 10, 11, 12, 13, 14\}$ while maintaining $\gamma_1 = 0.52$, and $\gamma_2 = 0.083$. As one

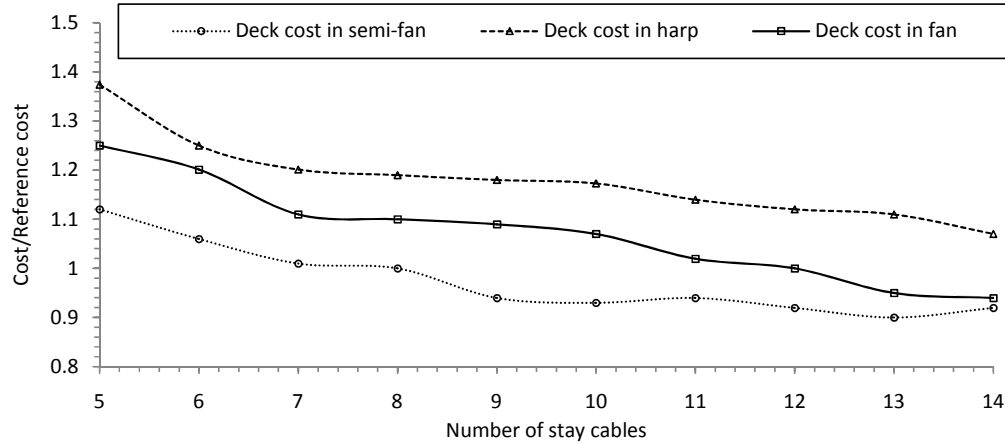


Figure 3.15: Variation of deck cost with number of stay cables in three types of cable-stayed bridges. Note that $N = \{5, 6, 7, 8, 9, 10, 11, 12, 13, 14\}$, $\gamma_1 = 0.52$, and $\gamma_2 = 0.083$

can see in this figure, the cost of the pylon increases linearly as the number of stay cables increases. As the number of stay cables increases a higher pylon is required to accommodate the cable anchor positions on the pylon.

3.2.4.2 Effect of Number of Cables on the Deck Cost

The main span length (M), and the height of the pylon (H) are equal to the original values of the Quincy Bayview Bridge. The number of stay cables is chosen from $N = \{5, 6, 7, 8, 9, 10, 11, 12, 13, 14\}$. Increasing the number of stay cables consistently decreases the cost of the deck as shown in Fig. 3.15. This is due to the reduction in the bending moment leading to a decrease in the thickness of the deck and consequently a reduction in the cost of the deck. However, beyond a value of twelve stay cables in the the semi-fan and fan ($N = 13$) arrangements, the increase in the deck cost becomes very small. Note that applying more than twelve cables results in a decrease in the deck cost in the harp arrangement. It should be noted that the reduction is remarkable only for increasing the number of stay cables from 5 to 8. It is worth mentioning that increasing the number of stay cables more than 8 is not very efficient for all arrangements hence should not be considered. If one compares these three

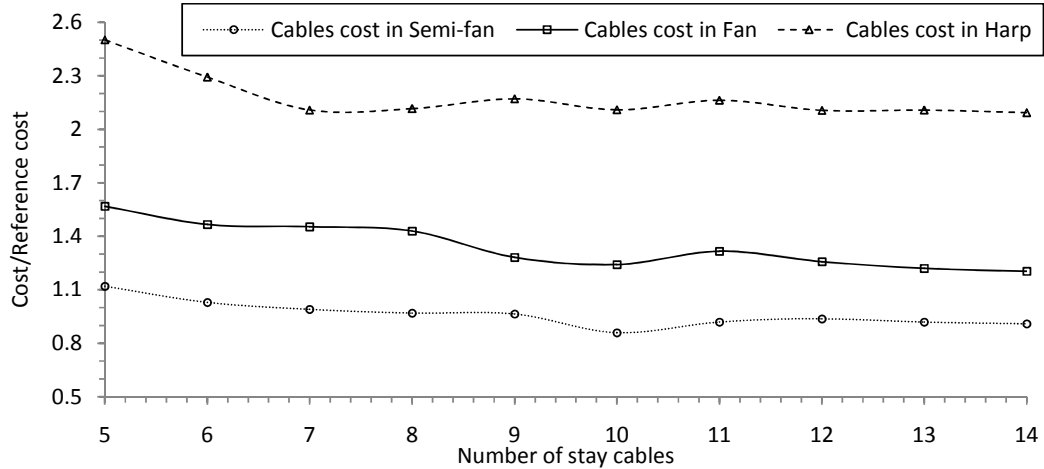


Figure 3.16: Variation of cables cost with number of stay cables in three types of cable stayed-bridges. Note that $N = \{5, 6, 7, 8, 9, 10, 11, 12, 13, 14\}$, $\gamma_1 = 0.52$, and $\gamma_2 = 0.083$

arrangements to each other, as seen in Fig. 3.15, the harp arrangements has the highest deck cost.

3.2.4.3 Effect of Number of Cables on the Cables Cost

In Fig. 3.16, the variation of cables cost with the number of stay cables $N = \{5, 6, 7, 8, 9, 10, 11, 12, 13, 14\}$ for the three arrangements is illustrated. As seen, harp arrangements has more cable cost in comparison to the other two arrangements. Note that semi-fan has the least cables cost.

3.2.4.4 Effect of Number of Cables on the Bridge Cost

In Fig. 3.17, the variation of the total cost of the bridge with the number of stay cables for the three cable arrangements is illustrated. The total cost of the bridge increases when the number of stay cables increases more than 10 in semi-fan arrangement. In comparison to the fan type, the total cost of the bridge is higher for the harp arrangement and, as expected, the semi-fan arrangement has the lowest cost in comparison to the two other arrangements.

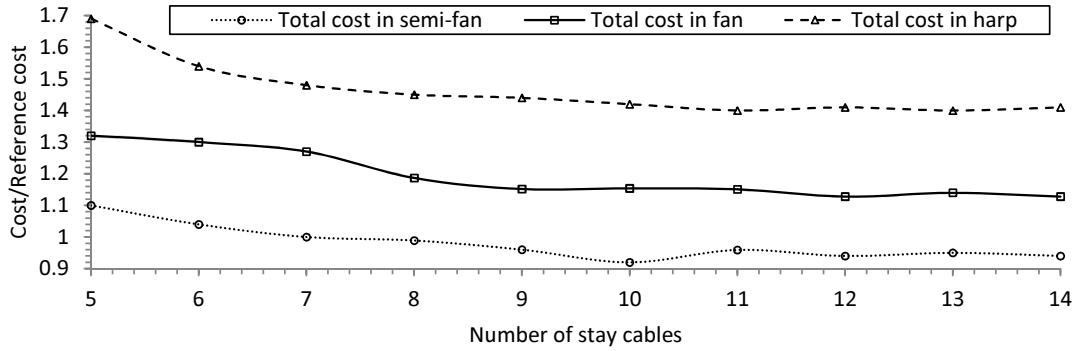


Figure 3.17: Variation of total cost with number of stay cables in three types of cable-stayed bridges. Note that $N = \{5, 6, 7, 8, 9, 10, 11, 12, 13, 14\}$, $\gamma_1 = 0.52$, and $\gamma_2 = 0.083$

3.3 Conclusions

In this study, an implementation of an efficient optimization method in the design of the cable-stayed bridges have been introduced considering fan and harp arrangements. The optimum cost design for three types of cable-stayed bridges are compared with each other and the result of comparisons are reported. First, a numerical model based on finite element model is developed for two fan and harp arrangements of cable stayed bridges. Then, based on the finite element model, real coded genetic algorithm, and three dimensional linear interpolation, the optimum design costs are obtained. The effect of various geometrical parameters on the the different bridge components are investigated for fan and harp arrangements and are compared to the semi-fan arrangement. At the end, the total optimum cost of all these three arrangements are compared to each other. The results indicated that the optimum total cost of the semi-fan arrangement is less than the two other arrangements. The specific conclusions that can be drawn from this chapter are numerated as follows:

- The design cost of the cable-stayed bridges is significantly affected by the variations of the geometrical parameters specifically height of the pylon above the deck and the mid-span length for all arrangements. Hence, these two parameters

should be considered within the design variables.

- The variation of the number of cables has considerable effect on the design cost of cable stayed bridges. Increasing the number of cables increases the cost of the pylon and reduces the cost of the deck. Accordingly, the number of stay cables are required to be included within the set of design variables.
- The increase in the pylon height reduces the optimum deck cost for three arrangements of cable stayed bridges. Moreover, the optimum deck cost reduces as the mid-span length reduces. Further, the variation of geometric configurations has more impact on the optimum deck cost for the harp arrangement.
- After applying post-tensioning forces to the stay cables on the fan and harp arrangements, the total costs are comparable to the cost of the reference bridge (semi-fan obtained by Hassan (2010)). One should note that without considering the post-tensioning cable forces, the total cost of the fan and harp arrangements are expected to be very high.

Bibliography

- M. Hassan. *Optimum Design of Cable-Stayed Bridges*. PhD thesis, The University of Western Ontario, 2010.
- John. Wilson and Wayne Gravelle. Modelling of A Cable-Stayed Bridge For Dynamic Analysis. *Journal of Earthquake Engineering and Structural Dynamics*, 20:707–771, 1991.
- M.M. Hassan, A. A. El Damatty, and Nassef. Determination of Optimum Post-Tensioning Cable Forces for Cable-stayed Bridges. *Journal of Engineering Structures*, in press, 2012.
- H. Bernard, Isler Walmer, and Moia Pierre, editors. *Cable Stayed Bridges*. Presses Polytechniques Romandes, Lausanne, Switzerland, 1988. ISBN 0-7277-1321-3.
- K. Tori, K. Ikeda, and T Nagasaki. A Non-iterative Optimum Design Method for Cable-Stayed Bridges. In *Proceedings of Japan Society of Civil Engineers*, pages 115–123, 1968.
- LMC. Simoes and JHJO Negroao. Sizing and Geometry Optimization of Cable-stayed Bridges. *Journal of Computer and Structure*, 52:309–321, 1994.
- W.X. Ren and X.L. Peng. Baseline finite element modeling of a large span cable-stayed bridge through field ambient vibration tests. *Computers & structures*, 83(8):536–550, 2005.

- F. Nieto, S. Hernandez, and J A. Julardo. Optimum Design of Long-span Suspension Bridges Considering Aeroelastic and Kinematic Constraints. *Journal of Structure Multidisc. Optim.*, 39:133–151, 2009.
- W. Long, MS. Troitsky, and ZA Zielinski. Optimum Design of Cable Stayed Bridges. *Journal of Structural Engineering and Mechanics*, 7:241–257, 1999.
- LMC. Simoes and JHJO Negro. Optimization of Cable-Stayed Bridges with Box-girder Decks. *Journal of Advanced Engineering*, 31:417–423, 2000.
- D. Jajnic, M. Pircher, and H Pircher. Optimization of Cable Tensioning in Cable-Stayed Bridges. *Journal of Bridge Engineering*, 8:131–137, 2003.
- YU-CHi. Sung, Dyi-Wei. Chang, and Eng-Huat Teo. Optimum Post-Tensioning cable Forces of Manu-Lo Hsi Cable-Stayed Bridge. *Journal of Engineering Structures*, 28:1407–1417, 2006.
- T.Y. Lee, Y.H. Kim, and S.W. Kang. Optimization of tensioning strategy for asymmetric cable-stayed bridge and its effect on construction process. *Structural and Multidisciplinary Optimization*, 35(6):623–629, 2008.
- V. Lute, A. Upadhyay, and KK Singh. Computationally Efficient Analysis of Cable-stayed Bridges for GA-based Optimization. *Journal of Engineering Applied Artificial Intell.*, 22(4-5):750–758, 2009.
- A. Baldomir, S. Henandez, F. Nieto, and A Jurado. Cable Optimization of a Long Span Cable-Stayed Bridge in La Coura (Spain). *Journal of Advances in Engineering Software*, 41:931–938, 2010.
- Tao. Zhang and ZhiMin Wu. Dead Load Analysis of Cable-Stayed Bridge. In *International Conference on Intelligent Building and Management (CSIT'11)*, pages 270–274, 2011.

- PH. Wang, TC. Tseng, and CG Yang. Initial Shape of Cable Stayed Bridges. *Journal of Computational Structure*, (46):1095–1106, 1993.
- JH Ernst. Der E-Modul von Seilen unter berucksichtigung des Durchhanges. *Der Bauingenieur*, 40(2):52–59, 1965.
- AS. Nazmy and AM. Abdel-Ghaffar. Three-dimensional nonlinear static analysis of cable-stayed bridges. *Journal of Structural Engineering*, 34(2):257–271, 1990.
- W Jr Weaver and JM Gere, editors. *Matrix Analysis of Framed Structures*. 3rd Edn, New York: Van Nostrand Reinhold; 1980, 1980.
- M. Gen and R. Cheng, editors. *Genetic Algorithms and Engineering Optimization*. Wiley, NewYork, 2000. ISBN 0-7277-1321-3.
- M. Pourazaday and X. Xu. Direct Manipulations of B-spline and NURBS Curves. *Journal of Advances in Engineering Software*, 31(2):107–118, 2000.
- AM El Ansary, AA El Damatty, and AO Nassef. A coupled finite element genetic algorithm technique for optimum design of steel conical tanks. *Thin-Walled Structures*, 48(3):260–273, 2010.
- CAN/CSA-S6-06. Canadian highway bridge design code s6-06 (can/csa s6-06). *Canada: Canadian Standard Association, Ontario*, 2006.
- AASHTO.LRFD. Bridge Design Specifications. *4th Edition Washington D.C., USA*, 2007.
- L Davis, editor. *Handbook of Genetic Algorithms*. Van Nostrand Reinhold, New York, USA, 1991. ISBN 0-7277-1321-3.
- Z Michalewics and DB Fogel, editors. *How to Solve it: Modern Heuristics*. 2nd Edition, Springer, New York, USA, 2004.

R Walther, B Houriet, W Isler, P Moia, and JF Klein. Cable-Stayed Bridges. *Thomas Telford Ltd*, 1988.

MS Troitsky, editor. *Cable-Stayed Bridges: Theory and Design*. 2nd Edition, Oxford: BSP 1988, 1988.

Chapter 4

Summary of the Thesis

4.1 Thesis Contributions

IN this study, a comprehensive structural evaluation and design optimization of cable-stayed bridges has been performed. The three main arrangements of cable-stayed bridges including, fan, semi-fan, and harp arrangements have been considered. This includes an evaluation of the post-tensioning cable forces and comparison between the forces associated with each arrangement. A comprehensive optimization procedure, that considers all the geometric and cross section parameters that define cable-stayed bridges is conducted for the three configurations.

- In Chapter 1, background information is provided about cable-stayed bridges for three main arrangements. Also, the history of employing post-tensioning cable forces for the optimal design of cable stayed bridges is reviewed. Furthermore, current techniques to optimize three arrangements of cable-stayed bridges including harp, fan, and semi-fan are presented. The previous work available in the open literature have also been presented and described in this chapter.
- In Chapter 2, first, finite element models of three types of cable-stayed bridges, i.e., fan, semi-fan, and harp arrangements are provided. Then, the post-tensioning

cable forces for these two types of cable-stayed bridges are obtained based on the recent work proposed by Hassan et al. (2012). B-spline curves are employed to represent the distribution of cable forces along the deck length for these three arrangements. Therefore, the complexity of the optimization search space and as well as the computational time have been reduced. This method also increases the probability of finding the global optimum solution and improves the performance of the optimization technique. The determined post-tensioning cable forces are compared to the one obtained for the semi-fan arrangement reported by Hassan et al. (2012). The effects of variation of upper strut height (pylon height), mid-span length, and the number of stay cables, on the post-tensioning cable forces have been investigated. The following conclusions can be stated from this part of the thesis as:

1. The variation of height of the pylon has a significant effect on the post-tensioning cable forces in all three arrangements. This is more pronounced in the inner stay cables for harp arrangements.
 2. The increase in the number of cables distributes the effect of dead load and reduces the post-tensioning cable forces.
 3. The post-tensioning cable forces increase as the mid-span length increases. Also, the post-tensioning cable force of the outer cables increases rapidly with the increase of the main span length.
 4. The post-tensioning cable forces have the highest value for the harp arrangements and the lowest value for the semi-fan arrangements. Fan arrangement lies between semi-fan and harp arrangements in terms of post-tensioning cable forces.
- In Chapter 3, the optimization of three-span composite deck cable-stayed bridges with the fan, semi-fan, and harp arrangement are considered. The design cost

of the cable-stayed bridges is significantly affected by the variations of the geometrical parameters specifically height of the pylon above the deck and the mid-span length for all the arrangements. Hence, these two parameters should be considered within the design variables. In this chapter, the design method has been investigated deeply to obtain the optimal design cost for the three styles of cable-stayed bridges. Comparisons between different arrangements has been provided. To date, this is the first comprehensive cost evaluation of three main types of cable-stayed bridges based on three main geometrical parameters of cable-stayed bridges, i.e., pylon height, mid-span length, and the number of stay cables. These parameters have been included in the design variables of the design of cable-stayed bridges. Comparison is conducted with a reference bridge design. This reference bridge is obtained throughout an optimization of cross section of the Quincy Bayview bridge, in which the pylon height, number of cables, and mid-span length are kept unchanged. The following conclusions can be drawn from this part of the study as:

1. The variation of the number of stay cables has a considerable effect on the design cost of cable stayed bridges. Increasing the number of cables increases the cost of the pylon and reduces the cost of the deck. Accordingly, the number of stay cables are required to be included within the set of design variables.
2. Increasing the pylon height results in a reduction in the optimum deck cost for three arrangements of cable stayed bridges. The optimum deck cost reduces as the mid-span length reduces. Further, the variation of geometric configurations has more impact on the optimum deck cost for the harp arrangement.
3. After applying post-tensioning forces to the stay cables on the fan and harp arrangements, the total costs are 3% and 26% more than the cost for the reference bridge (semi-fan, presented by Hassan (2010)), respectively.

4. The semi-fan arrangement requires the least cost for the design and the harp arrangement is the most costly arrangement in comparison to the fan and semi fan arrangements.
5. The harp arrangement is not very efficient since it needs more steel for the cables as it provides large forces for the cables. It is suitable only for the short to medium long span bridges. Attaching more cables to anchorages in fan arrangement is challenging. Fan arrangement is suitable for medium to short span bridges with the limited number of stay cables. As expected, the semi-fan is considered to be the best solution.

4.2 Future Work

As future works, for this thesis, the following can be pursued.

- Recently, different types of decks are employed for cable-stayed bridges. It is promising to employ the optimization methods presented in this thesis for different types of decks.
- Conduct optimization method for long span suspension bridges.
- Finally, one can work on optimal cost design of cable-stayed bridges during construction.

Bibliography

- M. Hassan. *Optimum Design of Cable-Stayed Bridges*. PhD thesis, The University of Western Ontario, 2010.
- John. Wilson and Wayne Gravelle. Modelling of A Cable-Stayed Bridge For Dynamic Analysis. *Journal of Earthquake Engineering and Structural Dynamics*, 20:707–771, 1991.
- M.M. Hassan, A. A. El Damatty, and Nassef. Determination of Optimum Post-Tensioning Cable Forces for Cable-stayed Bridges. *Journal of Engineering Structures*, in press, 2012.
- H. Bernard, Isler Walmer, and Moia Pierre, editors. *Cable Stayed Bridges*. Presses Polytechniques Romandes, Lausanne, Switzerland, 1988. ISBN 0-7277-1321-3.
- K. Tori, K. Ikeda, and T Nagasaki. A Non-iterative Optimum Design Method for Cable-Stayed Bridges. In *Proceedings of Japan Society of Civil Engineers*, pages 115–123, 1968.
- LMC. Simoes and JHJO Negroao. Sizing and Geometry Optimization of Cable-stayed Bridges. *Journal of Computer and Structure*, 52:309–321, 1994.
- W.X. Ren and X.L. Peng. Baseline finite element modeling of a large span cable-stayed bridge through field ambient vibration tests. *Computers & structures*, 83(8):536–550, 2005.

- F. Nieto, S. Hernandez, and J A. Julardo. Optimum Design of Long-span Suspension Bridges Considering Aeroelastic and Kinematic Constraints. *Journal of Structure Multidisc. Optim.*, 39:133–151, 2009.
- W. Long, MS. Troitsky, and ZA Zielinski. Optimum Design of Cable Stayed Bridges. *Journal of Structural Engineering and Mechanics*, 7:241–257, 1999.
- LMC. Simoes and JHJO Negro. Optimization of Cable-Stayed Bridges with Box-girder Decks. *Journal of Advanced Engineering*, 31:417–423, 2000.
- D. Jajnic, M. Pircher, and H Pircher. Optimization of Cable Tensioning in Cable-Stayed Bridges. *Journal of Bridge Engineering*, 8:131–137, 2003.
- YU-CHi. Sung, Dyi-Wei. Chang, and Eng-Huat Teo. Optimum Post-Tensioning cable Forces of Manu-Lo Hsi Cable-Stayed Bridge. *Journal of Engineering Structures*, 28:1407–1417, 2006.
- T.Y. Lee, Y.H. Kim, and S.W. Kang. Optimization of tensioning strategy for asymmetric cable-stayed bridge and its effect on construction process. *Structural and Multidisciplinary Optimization*, 35(6):623–629, 2008.
- V. Lute, A. Upadhyay, and KK Singh. Computationally Efficient Analysis of Cable-stayed Bridges for GA-based Optimization. *Journal of Engineering Applied Artificial Intell.*, 22(4-5):750–758, 2009.
- A. Baldomir, S. Henandez, F. Nieto, and A Jurado. Cable Optimization of a Long Span Cable-Stayed Bridge in La Coura (Spain). *Journal of Advances in Engineering Software*, 41:931–938, 2010.
- Tao. Zhang and ZhiMin Wu. Dead Load Analysis of Cable-Stayed Bridge. In *International Conference on Intelligent Building and Management (CSIT'11)*, pages 270–274, 2011.

- PH. Wang, TC. Tseng, and CG Yang. Initial Shape of Cable Stayed Bridges. *Journal of Computational Structure*, (46):1095–1106, 1993.
- JH Ernst. Der E-Modul von Seilen unter berucksichtigung des Durchhanges. *Der Bauingenieur*, 40(2):52–59, 1965.
- AS. Nazmy and AM. Abdel-Ghaffar. Three-dimensional nonlinear static analysis of cable-stayed bridges. *Journal of Structural Engineering*, 34(2):257–271, 1990.
- W Jr Weaver and JM Gere, editors. *Matrix Analysis of Framed Structures*. 3rd Edn, New York: Van Nostrand Reinhold; 1980, 1980.
- M. Gen and R. Cheng, editors. *Genetic Algorithms and Engineering Optimization*. Wiley, NewYork, 2000. ISBN 0-7277-1321-3.
- M. Pourazaday and X. Xu. Direct Manipulations of B-spline and NURBS Curves. *Journal of Advances in Engineering Software*, 31(2):107–118, 2000.
- AM El Ansary, AA El Damatty, and AO Nassef. A coupled finite element genetic algorithm technique for optimum design of steel conical tanks. *Thin-Walled Structures*, 48(3):260–273, 2010.
- CAN/CSA-S6-06. Canadian highway bridge design code s6-06 (can/csa s6-06). *Canada: Canadian Standard Association, Ontario*, 2006.
- AASHTO.LRFD. Bridge Design Specifications. *4th Edition Washington D.C., USA*, 2007.
- L Davis, editor. *Handbook of Genetic Algorithms*. Van Nostrand Reinhold, New York, USA, 1991. ISBN 0-7277-1321-3.
- Z Michalewics and DB Fogel, editors. *How to Solve it: Modern Heuristics*. 2nd Edition, Springer, New York, USA, 2004.

R Walther, B Houriet, W Isler, P Moia, and JF Klein. Cable-Stayed Bridges. *Thomas Telford Ltd*, 1988.

MS Troitsky, editor. *Cable-Stayed Bridges: Theory and Design*. 2nd Edition, Oxford: BSP 1988, 1988.

Curriculum Vitae

Name: Olfat Sarhang Zadeh

Post-secondary Education and Degrees: Western University
M.E.Sc., London, Canada

Sharif University of Technology
M.Sc., Tehran, Iran

Azarbaijan Shahid Madani University
B.Sc., Tabriz, Iran

Honors and Awards: MITACS Enterprise Award 2012.
Western Graduate Scholarship (WGRS) 2010-2012.
Society of Graduate Studies Bursary, 2010.

Related Work Experience: Graduate Research Assistant (2010-present)
Western University
Graduate Teaching Assistant (2010-present)
Western University
Civil Engineer (2008-2009)
FARAZAB Counsulting Engineers Co., Tabriz, Iran